Certificate for Geomatics

University of Geneva 2012

Estimation of salt diapirs influence on land surface temperature using Landsat images: insights from Zagros Orogen

Mortaza Pirouz

Supervisors :

Prof. Quoc-Hy Dao Prof. Alain Dubois

The Zagros Mountain Belt, Southern Iran

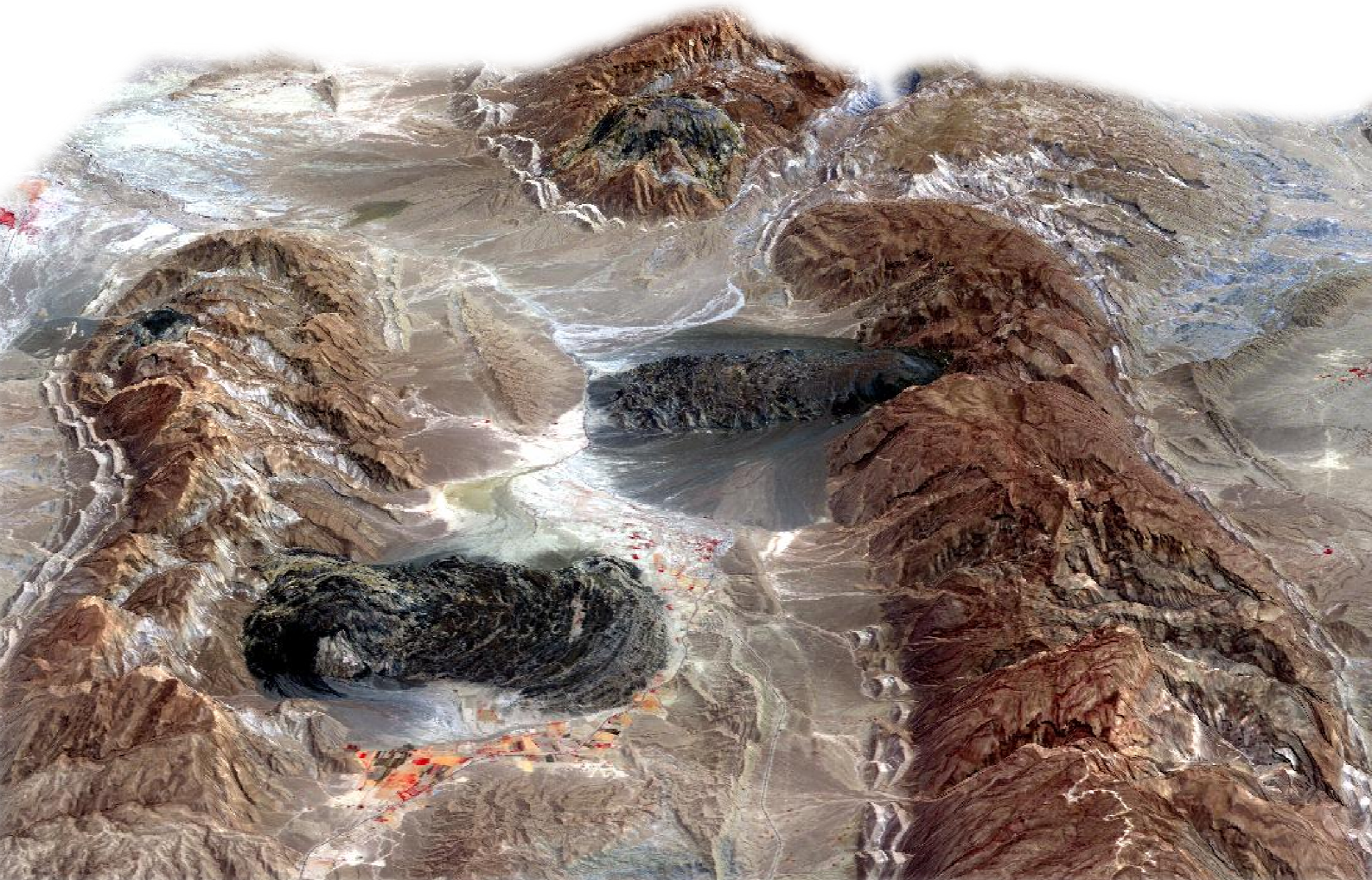

CONTENTS

ESTIMATION OF SALT DIAPIRS INFLUENCE ON LAND SURFACE TEMPERATURE USING LANDSAT IMAGES: INSIGHTS FROM THE ZAGROS OROGEN

Summary

The Zagros mountain belt is a part of the Alp-Himalayan chain. It is a result of the continent-continent collision between Arabian and Eurasian plates since Early Miocene (~20 Ma.). This region includes roughly about 12 km of sedimentary cover over the basement rock. This sedimentary cover decoupled from the basement rocks by Hormuz salt horizons. This salt unit has a thickness of the 2-4 km and extends mainly in the eastern sector of the Zagros. This Hormuz salt migrates upward and exposes at the surface as diapirs due to the regional contractional tectonic setting and its ductile behavior. The migration of the salt from minimum of 10 km depth to the surface causes heat transport to the surface and affects on the land surface temperature. The thermal band of the Tm and ETM satellite images are used to obtain temperature of the salt diapirs and their influence on the adjacent plains. Our result shows that salt diapirs have different temperature at the surface due to their different rate of activity. Temperature of the salt diapirs implies the amount of activity and extrusion. Our result shows that the salt diapirs in the northern part of the interior Fars region are 10 degrees warmer compared with southern alt diapirs. In addition, they have a large impact on the land surface temperature. The northern salt diapirs are located in higher altitude (~1200km) compared with southern salt diapirs. Although, the northern salt diapirs are located in the higher altitude and we expect to have colder surface temperature, but they are warmer due to their strong flow to the surface and high tectonic activity.

Keywords: *TM and ETM thermal band, Salt diapir, Land surface temperature, Zagros mountain belt*

1. INTRODUCTION

Land Surface Temperature (LST) is an extremely important parameter that controls the exchange of long wave radiation and sensible heat flux between the Earth's surface and the atmosphere. Therefore, knowledge of LST is essential for a range of issues and themes in Earth sciences central to hydrology, climatology and global environmental change.

The extreme heterogeneity of the land surface strongly depends on the air temperature and relative humidity, global solar radiation, wind speed and chemical and physical properties of the rocks. The role of the rocks becomes more efficient when there is a wide range of rocks with different physical properties and behaviors in response to the heat source. For instance,

the thermal conductivities of salt and evaporitic units are different from carbonate rocks. Indeed, different rock types with different physical properties can have large influence on the pattern of the land surface temperature. In addition, the amount of water into porous rocks such as sandstones and unconsolidated fluvial deposits would have different thermal properties in the valleys and flood plains.

In this study, we are interested to see the role of the salt in the land surface temperature, and the importance of the salt structures in the study area in details. We know that the salt has high thermal conductivity and therefore we expect that the salt diapirs have a large impact on the temperature of the surrounded area in our study area. These salts diapirs not only obtain the heat from the external sources, they also transport the heat from subsurface to surface by their upward movement and flow over the surface, which is the case in the Zagros region. The Zagros mountain region includes more than 220 salt diapirs, which are mostly active and include salt glaciers at the surface. These salt diapirs are mostly located in the eastern part of the Zagros region.

In this study, we investigate the influence of the salt diapirs on the land surface temperature and estimate relative extrusion rate of the salt diapirs. We consider the activity of the salt diapirs with regards to their relative warmth through a time. This is an important issue because of two main reasons. First, the land surface temperature can provide important information about the surface physical properties and climate which plays a role in many environmental processes (Dousset and Gourmelon, 2003; Weng et al., 2004), as an example we look at the distribution of villages in the study area as a consequence of this fact. Second, obtaining relative extrusion rate of the salt diapirs extrusion is not an easy task. It can be done by setting GPS stations and surveying, but it is expensive, unsafe (presence of invisible holes in the salt body) and time-consuming process. Remote sensing might be a better alternative to the aforesaid methods. The advantages of using remotely sensed data are the availability of high resolution, consistent and repetitive coverage and capability of measurements of earth surface conditions (Owen et al., 1998; Weng, 2009). It is important to emphasize that these salt diapirs are a potential for geothermal energy sources and they seal many oil and gas reservoirs in different depths, and therefore their thermal property and relative flow are important issues, which needs to be considered.

2. THE ZAGROS MOUNTAIN BELT

The Zagros mountains are the part of the Alpine-Himalayan chain that forms the northern margin of the Arabian plate (Takin, 1972; Berberian and King, 1981; Talbot and Alavi, 1996) and locates in the southern Iran. It is among the most famous geological provinces in the world, renowned for its spectacular whaleback anticlines, extreme seismic activity and presence more than 220 salt diapirs (Figures 1 and 2). The Zagros fold-thrust belt is currently shortening at a rate of 20 mm yr^{-1} (Sepehr and Cosgrove, 2004; Hessami et al., 2006; Hessami et al., 2006; Allen and Armstrong, 2008) and experiencing regional uplift of 1 mm yr^{-1} (Lees and Falcon, 1952; Falcon, 1974; Snyder and Barazangi, 1986; Tatar et al., 2002; Sepehr and Cosgrove, 2004; Hessami et al., 2006). The Zagros Mountains are currently extremely seismically active. This region is one of the world's richest

hydrocarbon provinces with 66.7% of the proven recoverable oil and 31.5% of proven gas reserves of the world (Murris, 1980; Beydoun, 1991).

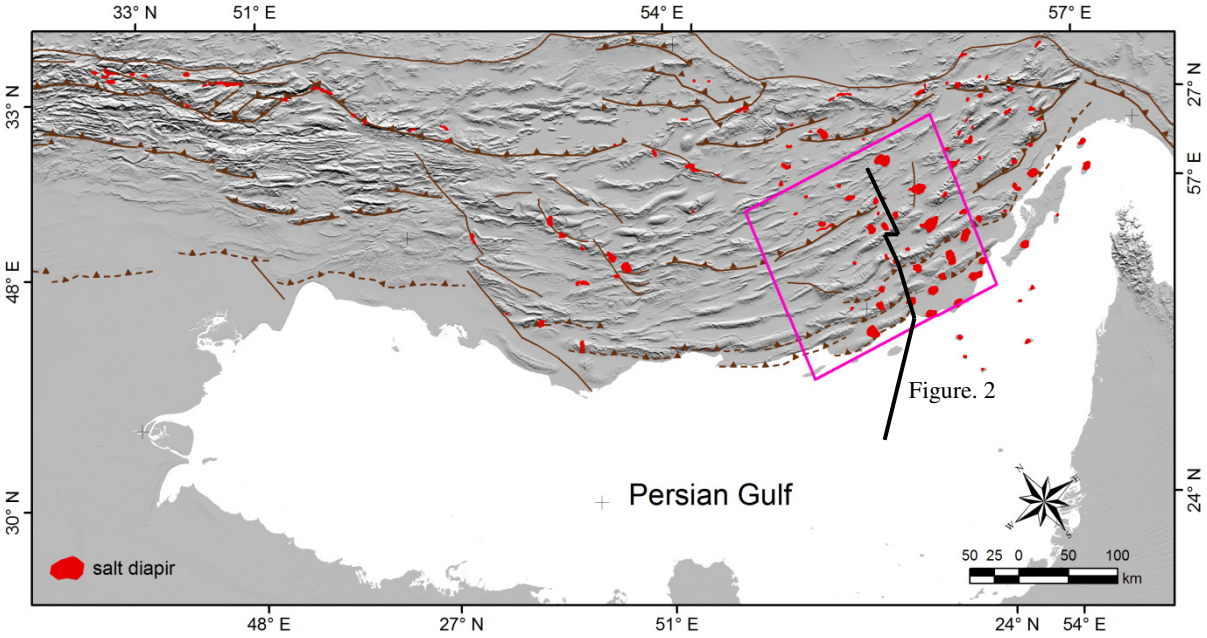

Figure 1. Digital elevation model of the Zagros Mountain belt. The salt diapirs (red polygons), major faults (brown lines) and the study area (pink polygon) are shown. Distribution map of the salt diapirs are digitized by the author using MrSid satellite images in ArcGIS. In addition, the base map is also are prepared in Global Mapper software using free Aster Global Digital Elevation Maps (http://asterweb.jpl.nasa.gov/gdem.asp).

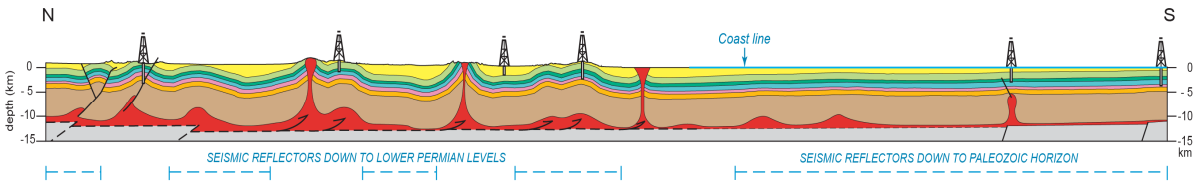

Figure 2. Structural section across the Zagros region on the basis of the seismic lines. Salt diapirs are shown in red, which are migrated to the surface from a depth of ~12km. The location of this section is shown in figure 1.

3. SALT DIAPIRS

Heat is critical for the occurrence of salt intrusion. Increased temperature greatly reduces the ultimate strength of salt and eliminates work hardening. When salt is heated above 205°C, it becomes soft and plastic and flows indefinitely with a pressure gradient of about 33-100 kg/cm^2 (460-1,400 psi) (Figure 3) (Gussow, 1968). It is plastic during the entire process of intrusion, and even during extrusion at the surface. Thus, at the time of extrusion, salt can flow by simple gravity, like a "glacier," as long as it remains hot. The source of the salt diapirs in the Zagros region is a thick salt horizon at depth of ~9 to ~13 km with ~400°C of temperature (by assuming increasing 30°C per 1 kilometer of depth and 30°C of surface temperature) (Figure 3). The Hormuz salt horizon decouples the basement rocks from the sedimentary cover and pierces the entire sedimentary cover by salt structures (Figure 2). These salt diapirs reach to the surface

and flow over the adjacent plains. These salt not only transport the subsurface heat with themselves to the surface also their high thermal conductivity let the salt bodies be warm through the geological time due to their connection to the basement rocks. Some of these diapirs in the Zagros region include hot springs and some of them warming up adjacent rivers. It is worth noting that the size of the salt diapirs is considerable and varies between several and 120 square kilometers in the Zagros region.

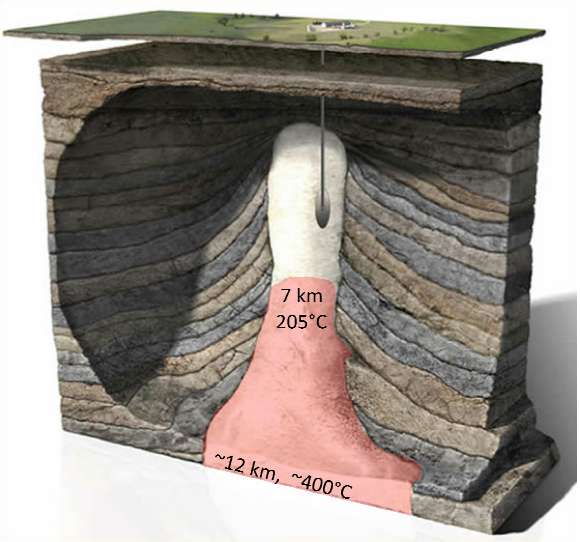

Figure 3. Schematic section of a salt diapirs. Temperatures in different depths are shown. The red zone shows that the salt is plastic and flows indefinitely with a pressure gradient of about 33-100 kg/cm^2.

3. THE STUDY AREA

In this study, we consider eastern part of the Zagros region (53.5°-55.5° E and 26.5°-28.5° N) where includes most of the salt diapirs. This region contains 36 of big salt diapirs of the entire Zagros region (Figure 1). This region has arid climate, very hot summers (between 38 and 50° C) and relatively warm winters (between 18 and 24°C). The annual rate of precipitation is almost zero in the extensive part of the study region. Topography level with a range of 2000 to 0 meters and different rock units are the only variables across the region.

4. SATELLITE DATA PROCESSING

The Landsat Thematic Mapper (TM) and Enhanced Thematic Mapper Plus (ETM+) sensors acquire temperature data and store this information as a digital number (DN) with a range between 0 and 255. It is possible to convert these DNs to degrees using two steps process. The first step is to convert the DNs to radiance values using the bias and gain values of the individual scene and the second step converts the radiance data to degrees. Satellite dataset of Landsat-5 (TM) and Landsat-7 (ETM+) over the study area of 13rd April 1987, 26nd May 2000 and 24nd March 2006 (day time, path/row 161/41) have been used in this study (cloud cover 0%). The single thermal band (6) of the TM and low gain single thermal band (6.1) of the ETM+ satellite images are used for this purpose. The satellite images and thermal bands of the study area were available in the Global Land Cover facility (GLCF) website and I downloaded these data via FTP server (ftp://ftp.glcf.umd.edu/glcf/Landsat/).

5. METHODOLOGY

5.1 CONVERT DN TO RADIANCE

GIS and remote sensing are used to develop the input data set for a conceptual model. In order to obtain land surface temperature maps from the TM and ETM+ images, we have calculated radiance maps at the first stage and later on convert them to degree maps by using different equations, which are

described in below. The formula to convert DN to radiance for TM images is:

$$CV_R = G\,(CV_{DN}) + B \qquad (1)$$

Where:

CV_R is the cell value as radiance

CV_{DN} is the cell value digital number

G is the gain

B is the bias (or offset)

The gain (G=0.05518) and bias (B=1.2378) (offset for TM) values are obtained from the *.met header file extension for the TM image.

The formula to convert DN to radiance for low gain band (6L) of ETM+ images is the same as equation (1), but with different G and B values. These values can be obtained from the header file with *.fst or *.met extensions. In addition these values for gain (G=0.067087) and bias (B= -0.07) can be used (Chander et al., 2009).

5.2 CONVERT RADIANCE TO DEGREE

Once the DNs for the thermal bands have been converted to radiance values, it is simply a matter of applying the inverse of the Planck function to derive temperature values (Schott and Volchok, 1985).

The formula to convert radiance to temperature (Celsius) is:

$$T = (K_2 / \mathrm{Ln}\,(((K_{1\times}\,\varepsilon)/CV_R) + 1)) - 273 \qquad (2)$$

Where:

T is degree, Celsius (°C)

CV_R is the cell value as spectral radiance in $Wm^{-2}sr^{-1}\mu m^{-1}$.

ε is emissivity (typically 0.95) (Buettner and Kern, 1965; Borel, 2008)

K1 and K2 are calibration constants.

The amount of the K_1 and K_2 are different in TM and ETM images and are written in below (table 1).

Table 1. Calibration constants for TM and ETM images

	Landsat TM	Landsat ETM
K1	607.76	666.09
K2	1260.56	1282.71

5.3 SURFACE ISOTHERM MAPS

In order to obtain the isotherm map for each individual image, several steps are followed. First of all the resolution of the obtained land surface temperature maps decreased from 60 to 500 with mean value of the previous cells using the *aggregate* (spatial analyst) tool in Arc GIS. At the next step, the new raster images converted to point by doing *Raster to point* and later on extrapolated to obtain the regional isotherm maps (Figure 4) by using *Geostatistical analyst* tools and *Local Polynomial Interpolation* method. The results let us to better understand land surface temperature isotherm patterns in order to locate thermal anomalies in the study area (Figure 5).

5.4 ATMOSPHERE ISOTHERM MAPS

The atmospheric isotherm maps are also obtained for the similar time period (years and months) for the study area using the statistical data of synoptic stations. These maps are calculated to compare with the land surface isotherm maps in order to see probable link between atmosphere heat and surface warmth. The statistical data are produced from digital elevation models by *Zonal Statistics* tool in GIS. The *Local Polynomial interpolation* is used for

interpolation purposes. Entire processes that are used in this study are shown in Figure 5.

5.5 CALIBRATION OF THE TEMPERATURES MAPS

However the temperature maps will be obtained by doing the previous steps which we already described them, but we need to calibrate the results with the real data which are measured in the field. We have used the temperatures of the Persian Gulf in different months as a key point to calibrate our final temperature maps. As shown in the figure 4, southern part of the images include northern coast of the Persian Gulf and a part of its water. The temperature of this part of the map is used for calibration and is applied for the rest of the study area.

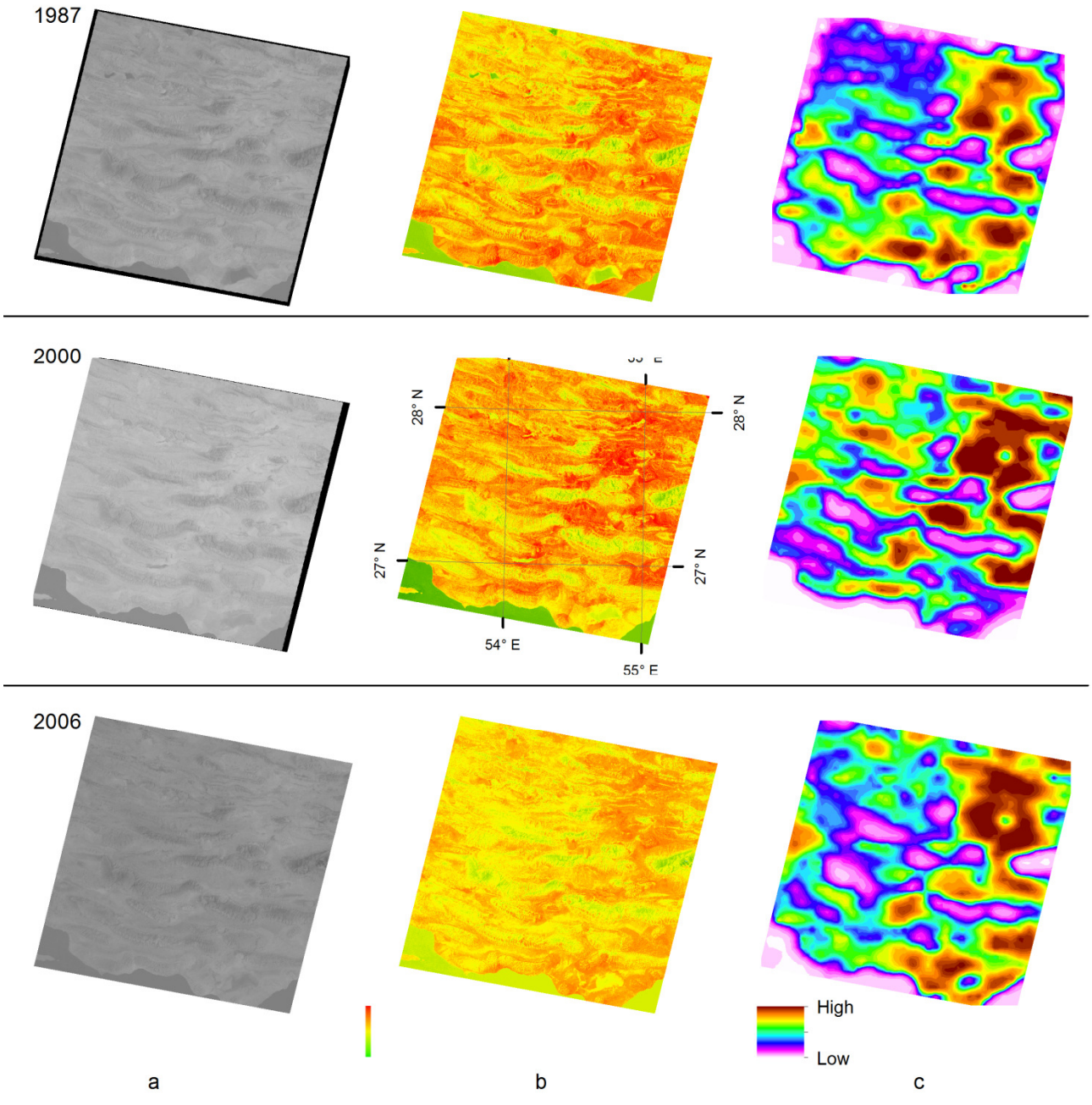

Figure 4. Satellite images (a), land surface temperature maps (b) and isotherm maps(c) of the study area derived from the 1987 TM, 2000 and 2006 ETM images.

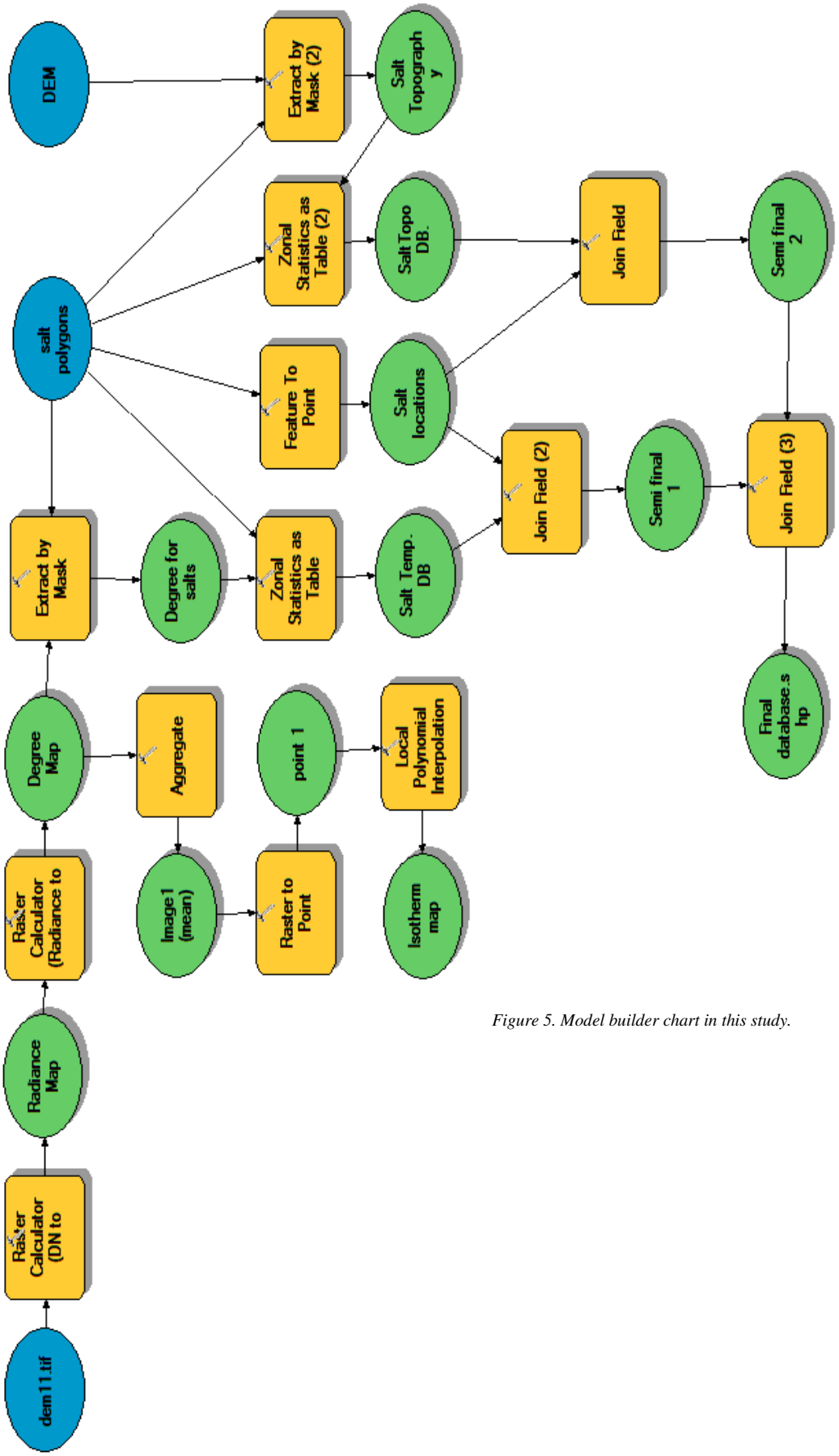

Figure 5. Model builder chart in this study.

6. RESULTS

6.1 LAND SURFACE AND SALT DIAPIRS TEMPERATURES

The land surface temperature (LST) map obtained from the Landsat TM (1987) shows a mean temperature range between 20 and 42.5°C degrees in April (Figure 6) with a 500 meters pixel resolution. The maximum LST with 42.5°C mostly is localized in the northeast and eastern part of the study area. The atmosphere temperature map based upon the measured statistical data of synoptic stations, which is shown in Figure 7 , has a range between 18 and 29°C degrees decreasing towards north for the April 1987. The mean and maximum temperature of the each individual salt diapirs in April 1987 are also considered (Figures 8 and 9). Salts diapirs have a mean temperature ranged from 31 to 43°C and a maximum range between 41 to 49°C with 500 and 60 meters of resolutions respectively.

The LST maps derived from ETM images for 2000 and 2006 images present that in May 2000, the surface temperature had a range between 30 to 56.5°C and temperature of the atmosphere between 20 and 35°C (Figure 10 and 11). At the same time, the salt diapirs show a mean range of temperature between 44 and 55°C and maximum range between 52.5 and 62 °C (Figures 12 and 13). Although, the land surface temperature had a range between 20 to 38°C degrees and atmosphere between 15 to 23°C in March 2006 (Figures 14 and 15). In addition, the salt diapirs show a mean temperature ranged from 27 to 38°C and maximum range between 37.5 and 46°C (Figures 16 and 17).

6.2 ELEVATION MAP OF THE AREA

Digital elevation model of the study area is obtained from SRTM[1] data, and the result presents that the northern part of the study area has higher altitude to compare with the southern coastal region approximately 1200 meters (Figure 18).

In addition, the elevation variables such as minimum, mean, maximum, range of topography of the diapirs are also calculated on the basis of the SRTM images with 25 meter pixel resolution (Figures 19, 20 and 21) and details are presented in Table 2. In general, the mean elevation of the diapirs increases towards north similar to the regional topography. These variables are extremely important morphological aspects. That is because they represent the relative amount of the extrusion and salt diapir actives. These variables along with morphological features (such as flow) and temperature let us to estimate the most active salt diapirs in the study area.

[1] Shuttle Radar Topography Mission

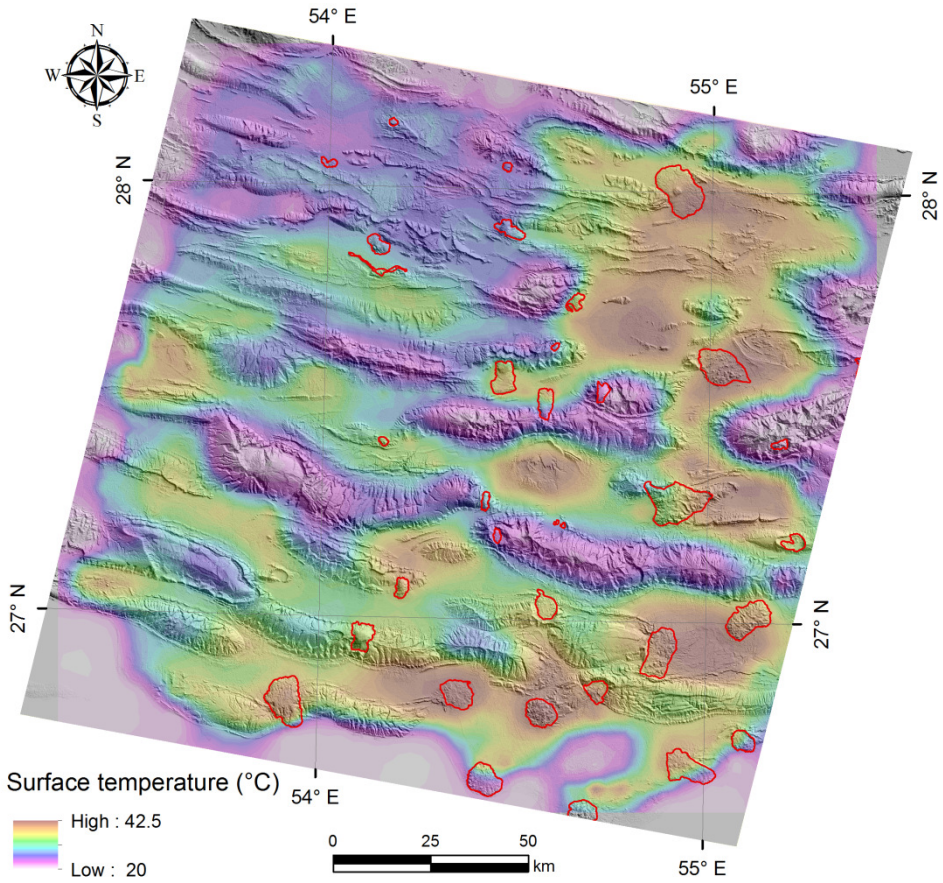

Figure 6. The surface isotherm map of the study area for April 1987.

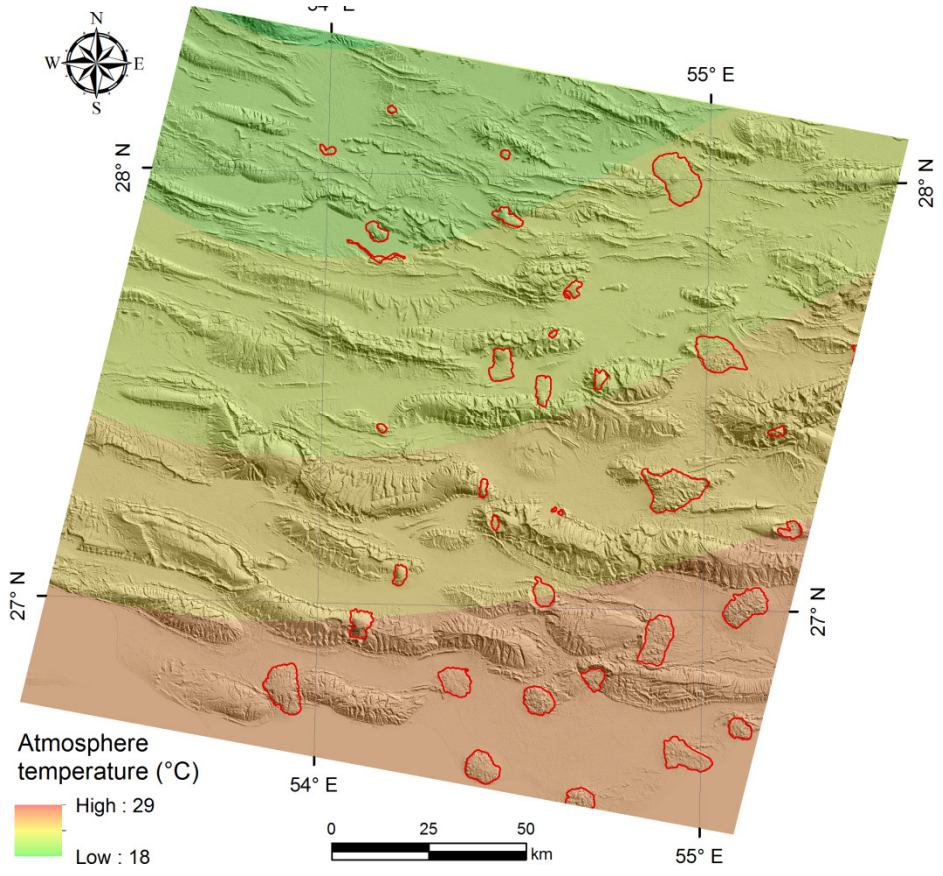

Figure 7. Temperature map of the atmosphere for the April 1987.

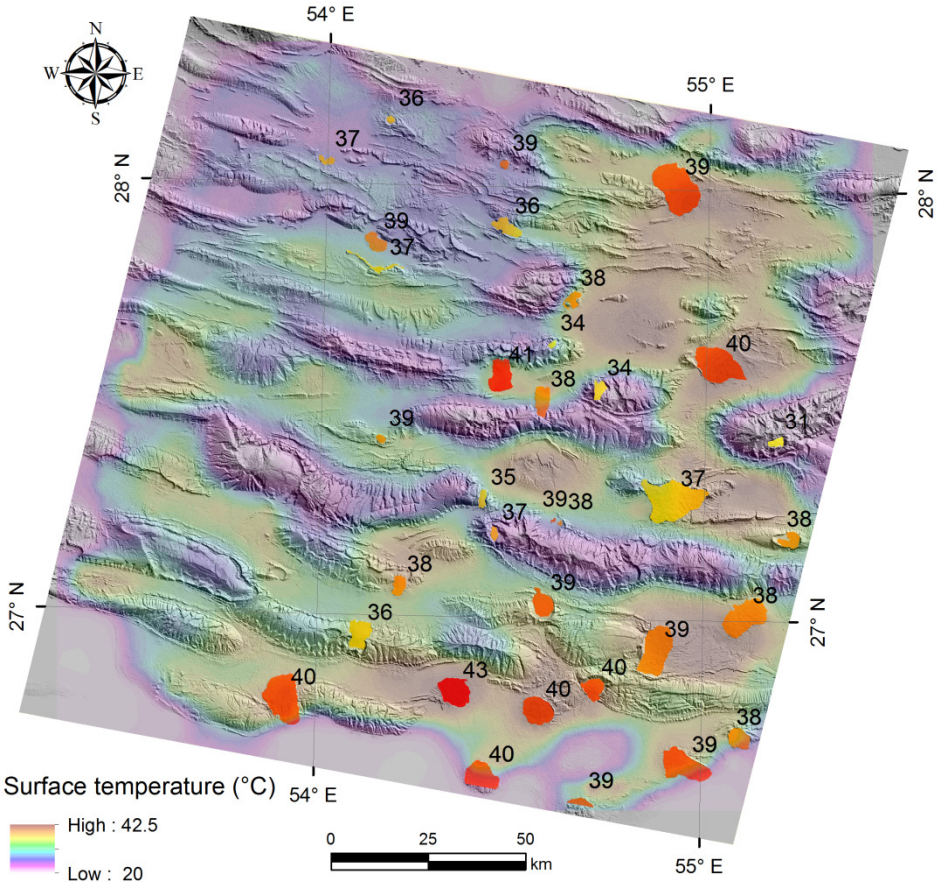

Figure 8. Mean temperature of the salt diapirs in the study area, April 1987.

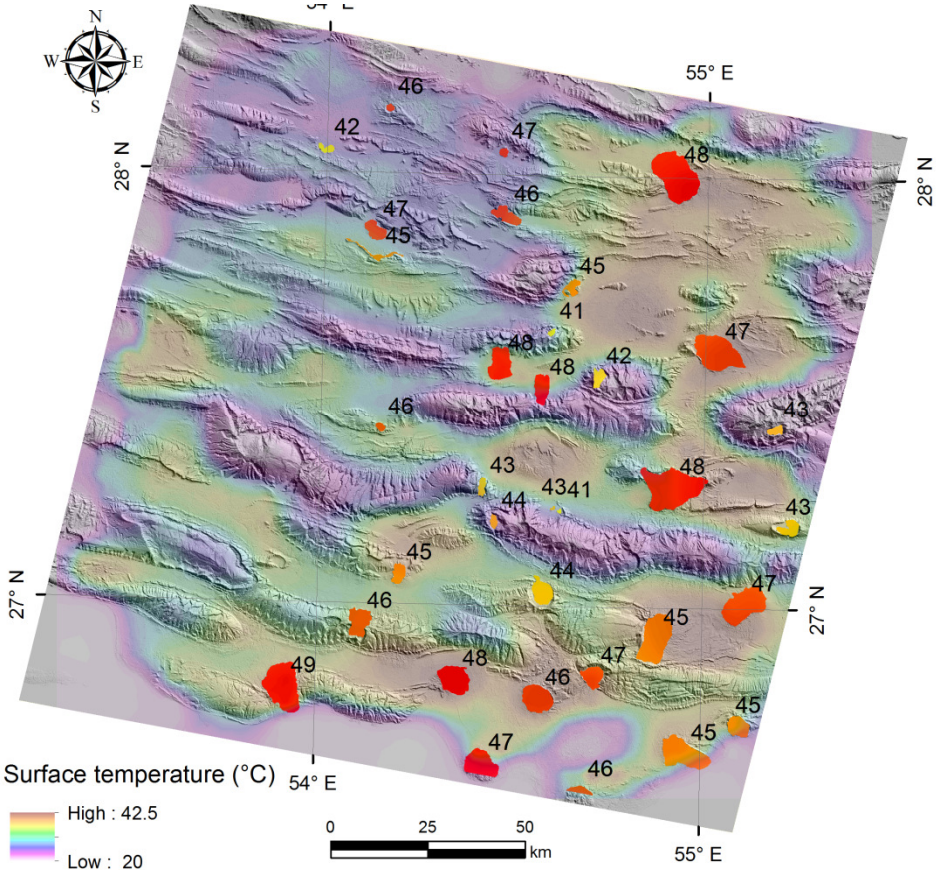

Figure 9. Maximum temperature of the salt diapirs in the study area, April 1987.

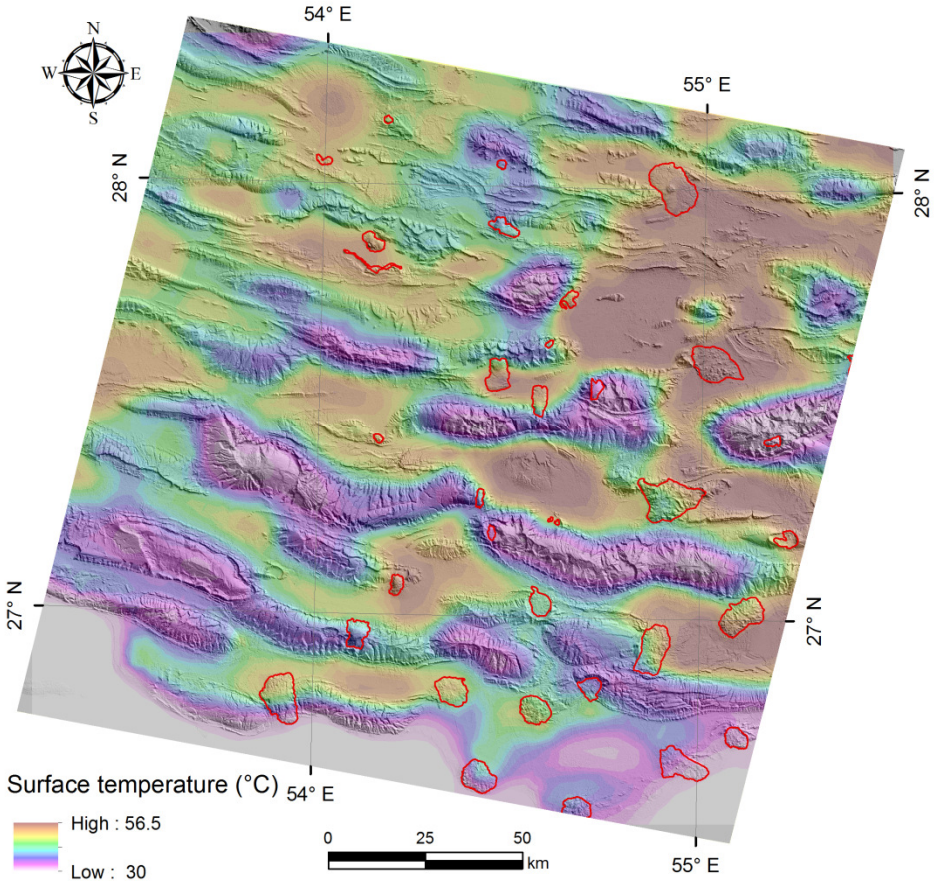

Figure 10. The surface isotherm map of the study area for May 2000.

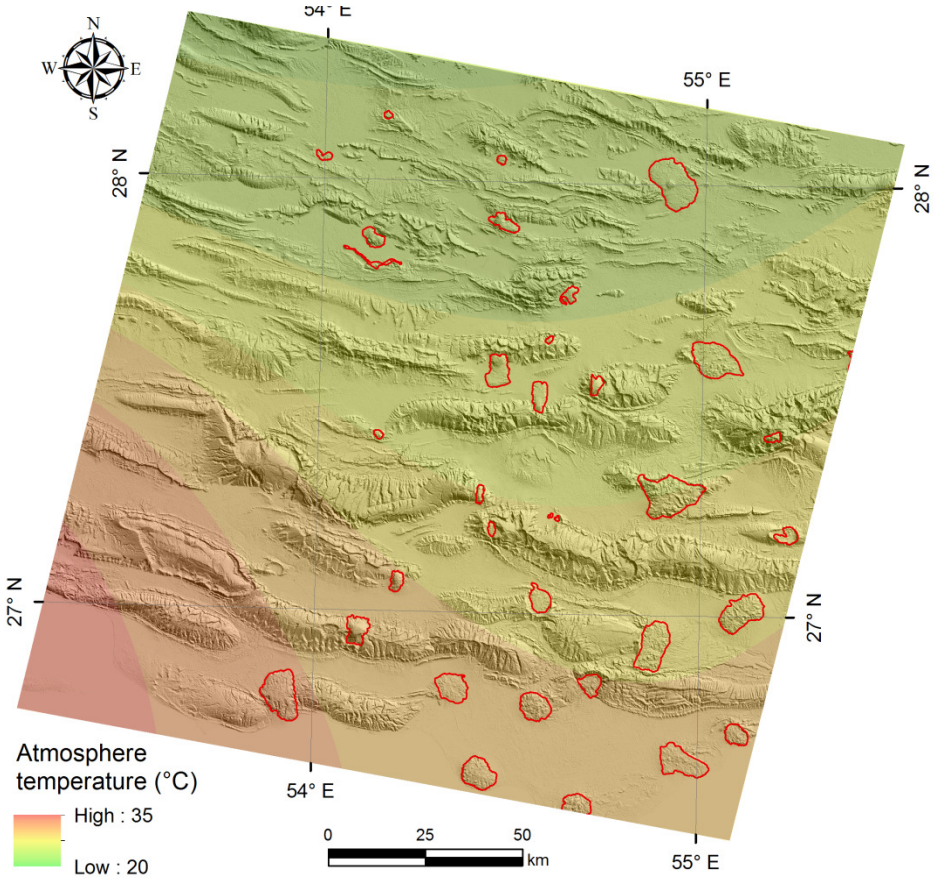

Figure 11. Temperature map of the atmosphere for the May 2000.

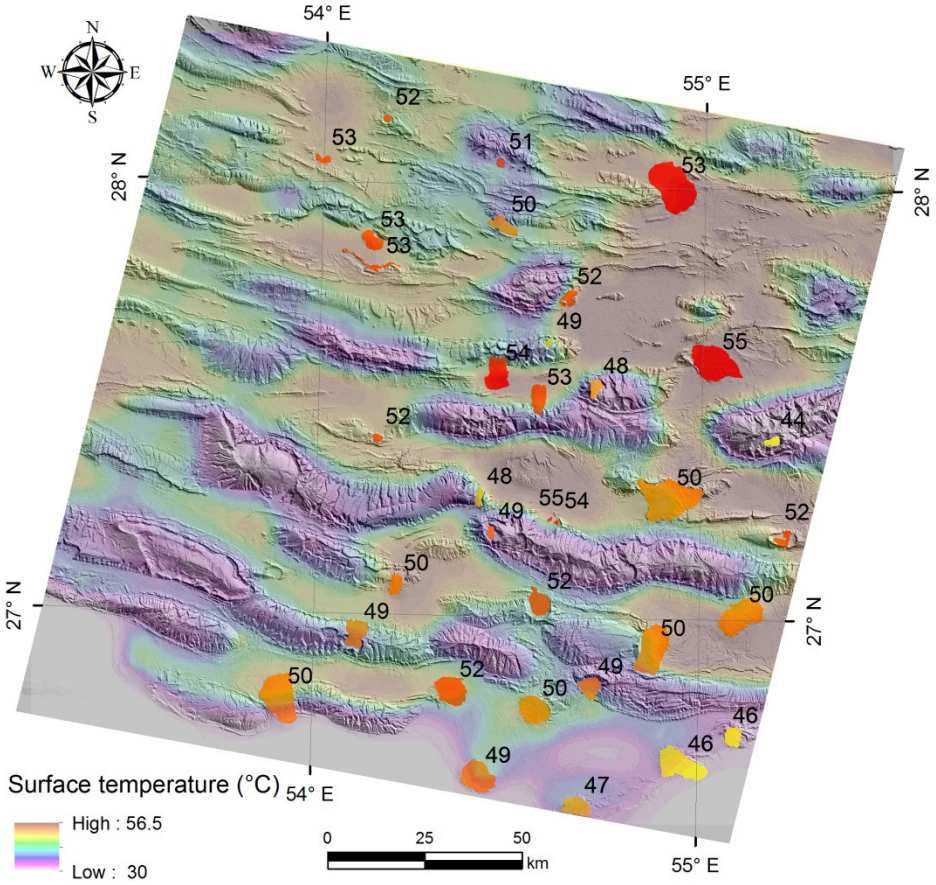

Figure 12. Mean temperature of the salt diapirs in the study area, May 2000.

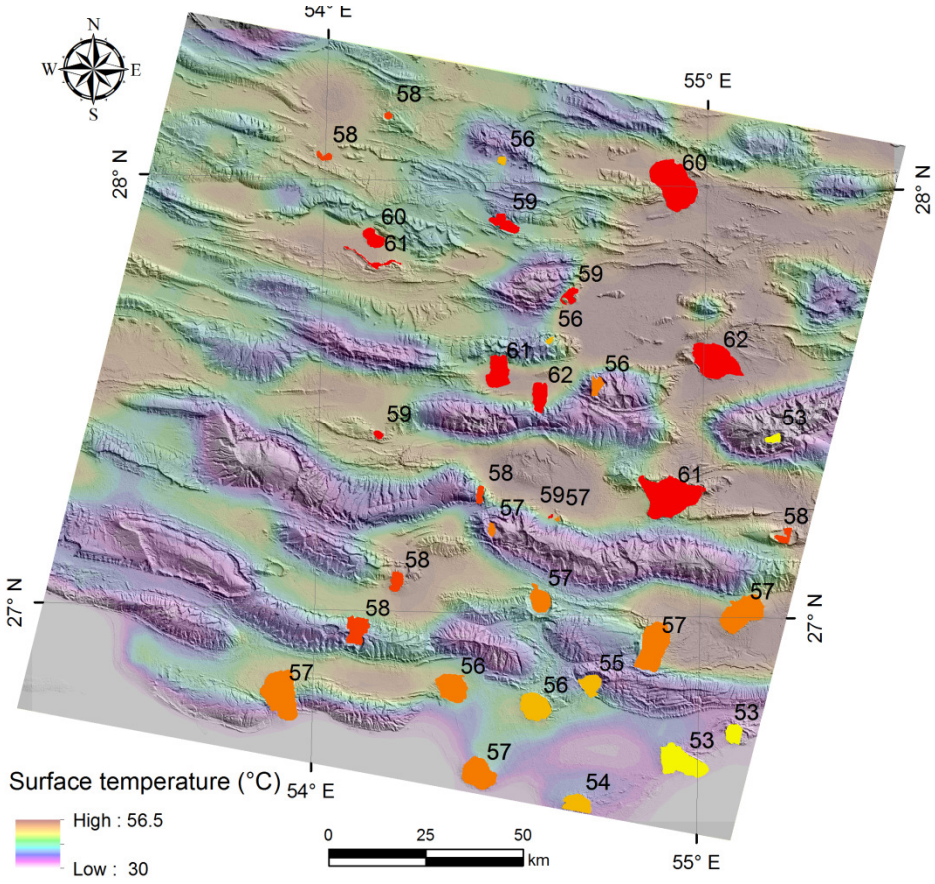

Figure 13. Maximum temperature of the salt diapirs in the study area, May 2000.

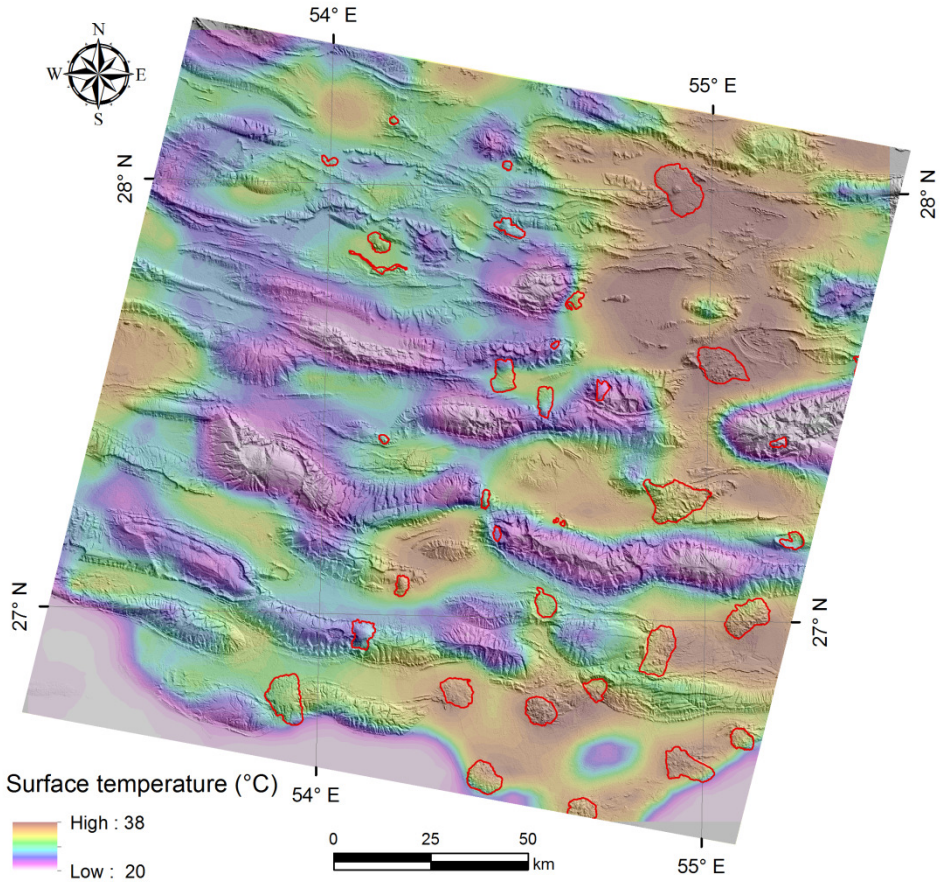

Figure 14. The surface isotherm map of the study area for March 2006.

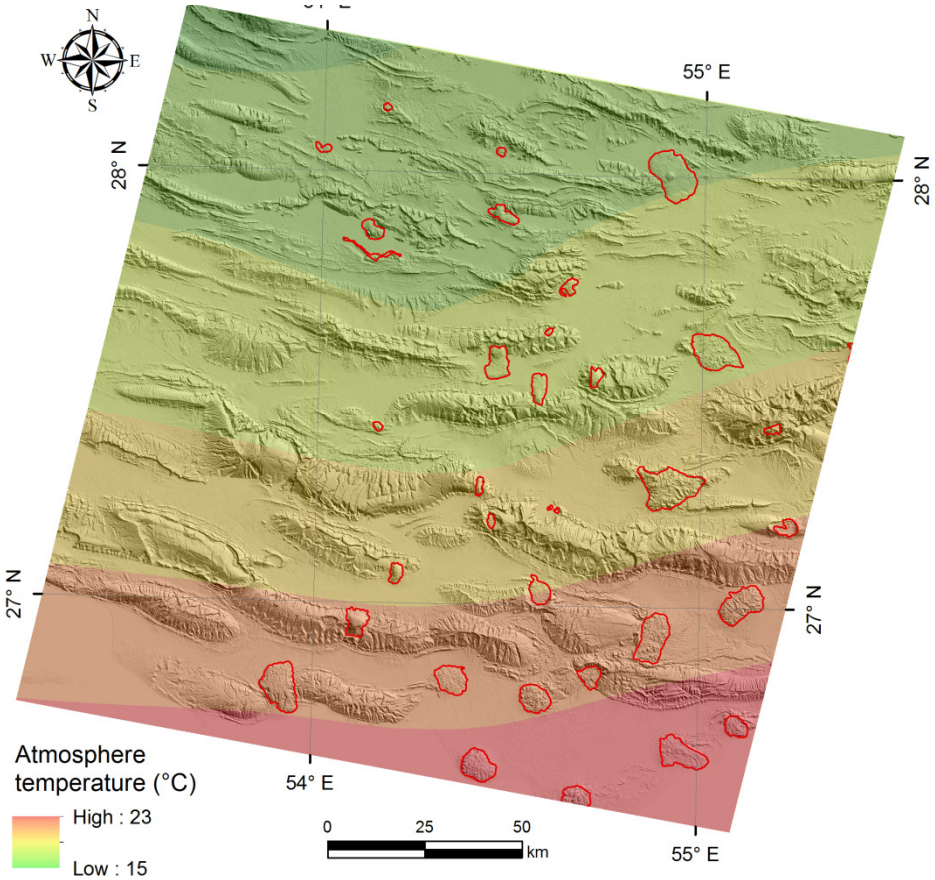

Figure 15. Temperature map of the atmosphere for the March 2006.

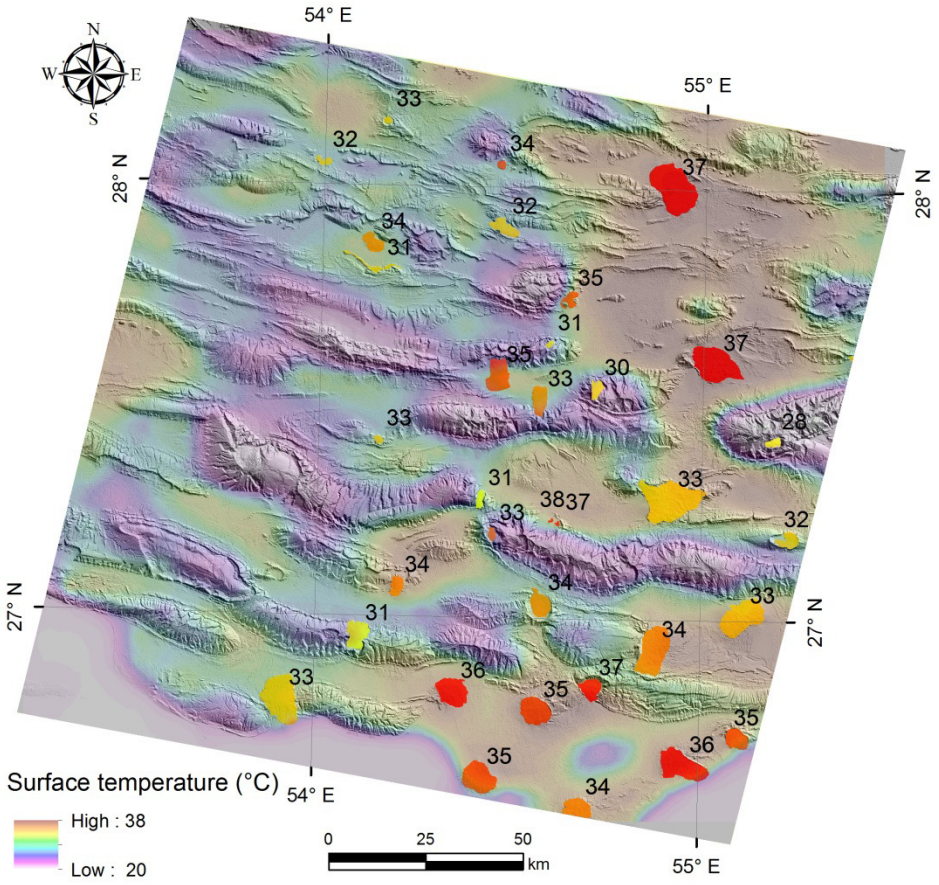

Figure 16. Mean temperature of the salt diapirs in the study area, March 2006.

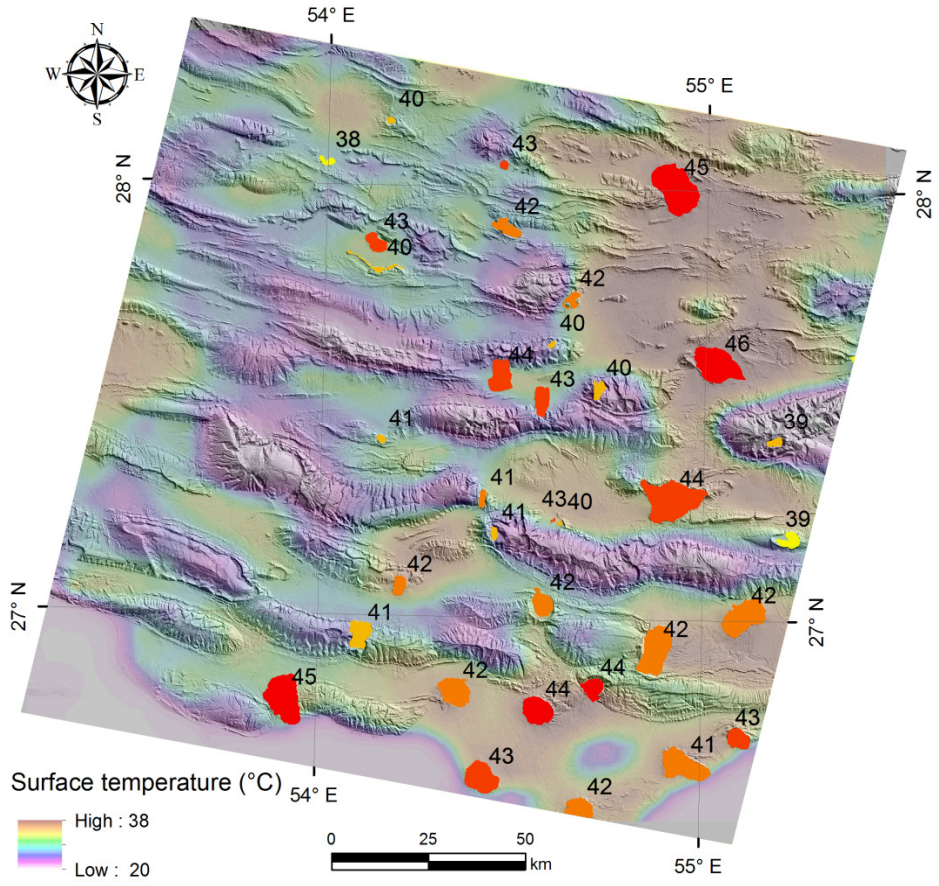

Figure 17. Maximum temperature of the salt diapirs in the study area, March 2006.

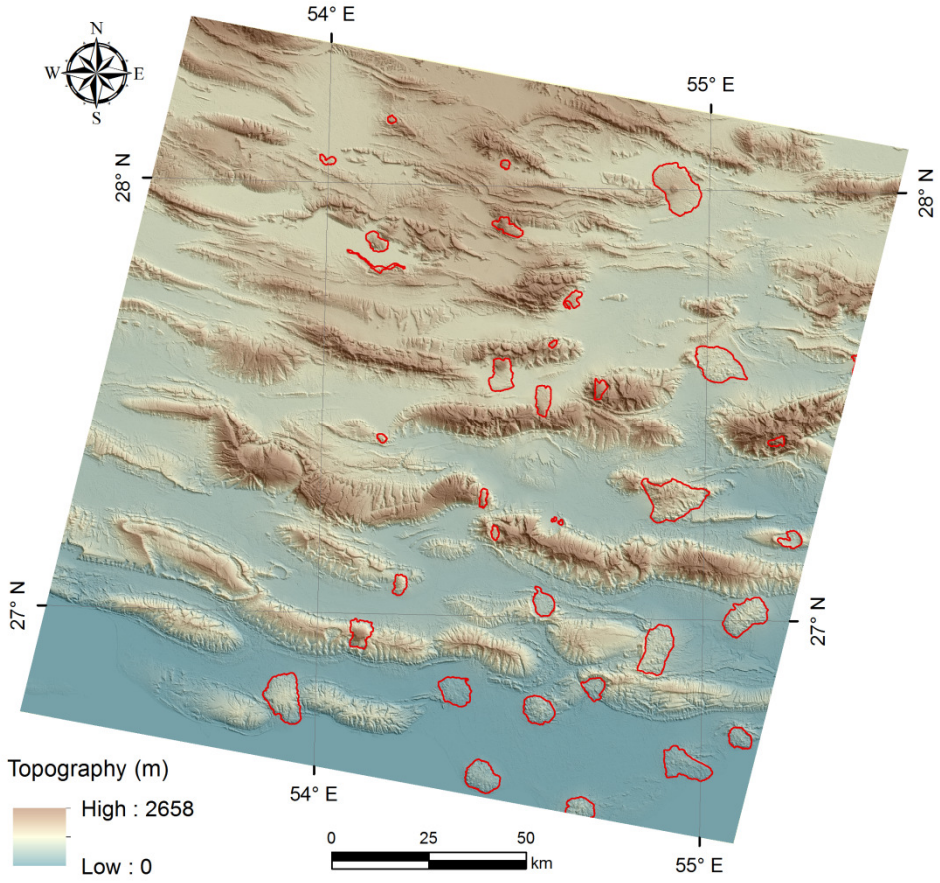

Figure 18. Digital elevation model of the study area on the basis of the SRTM data.

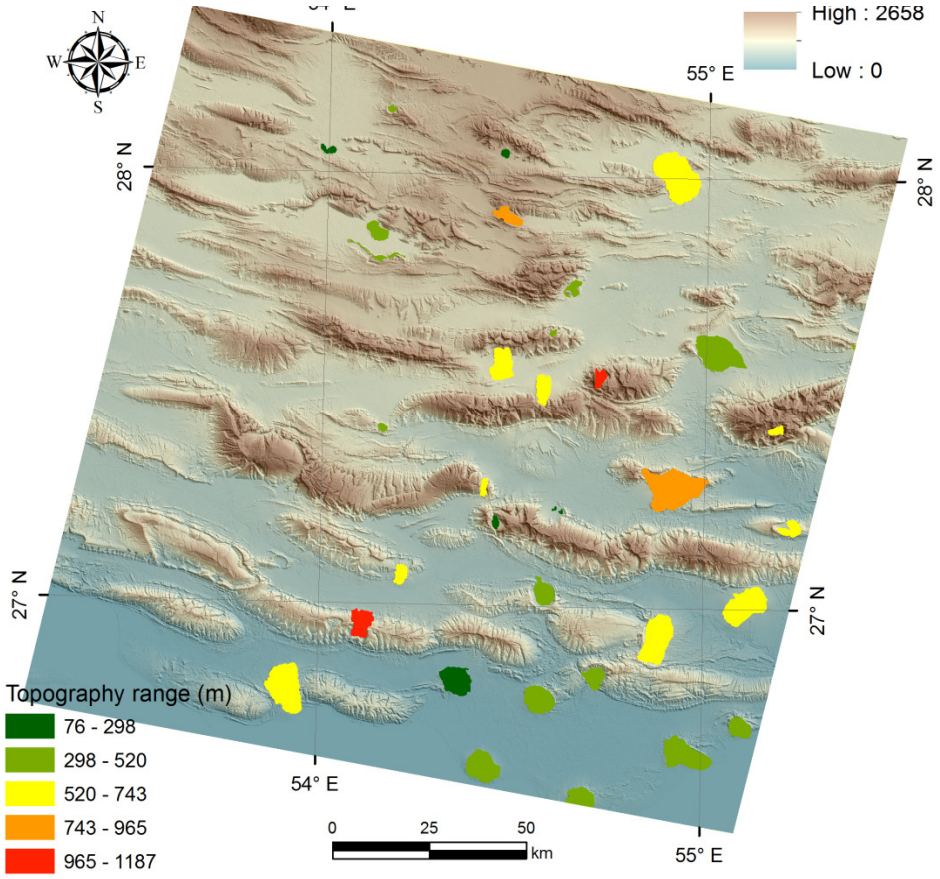

Figure 19. The height of the salt diapirs (topography range) in the study area. Increasing towards ~1000m of altitude

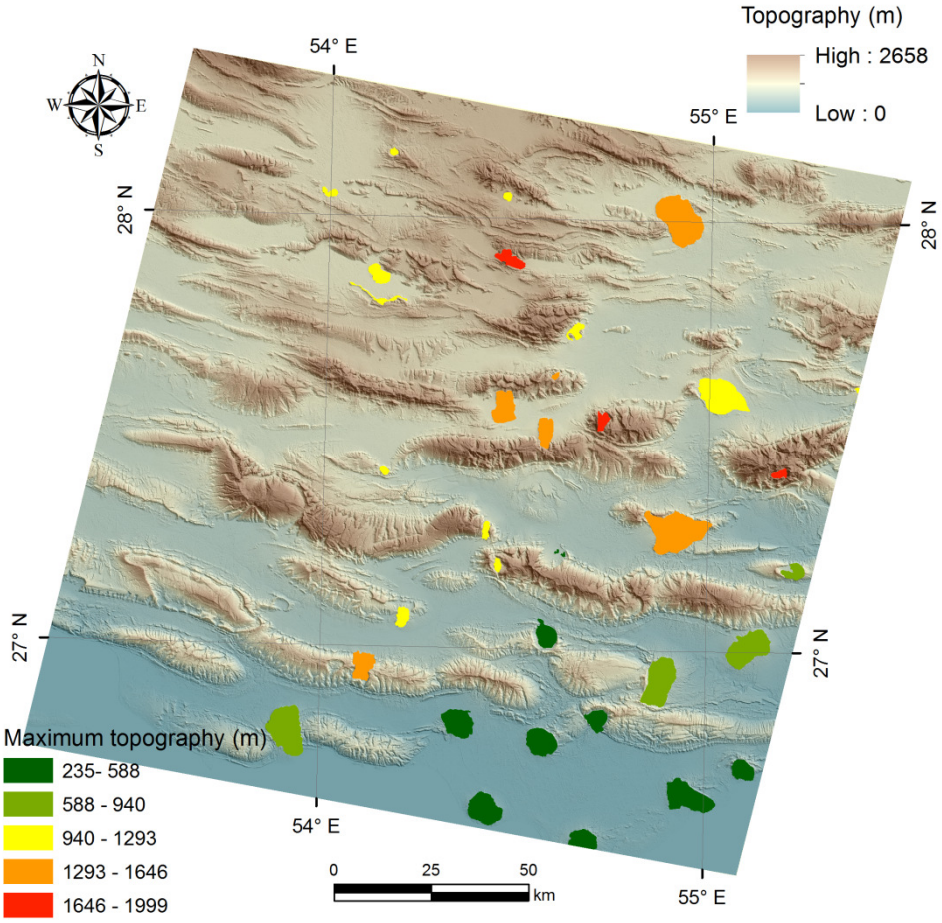

Figure 20. Maximum topography of the salt diapirs in the study area, increasing towards north.

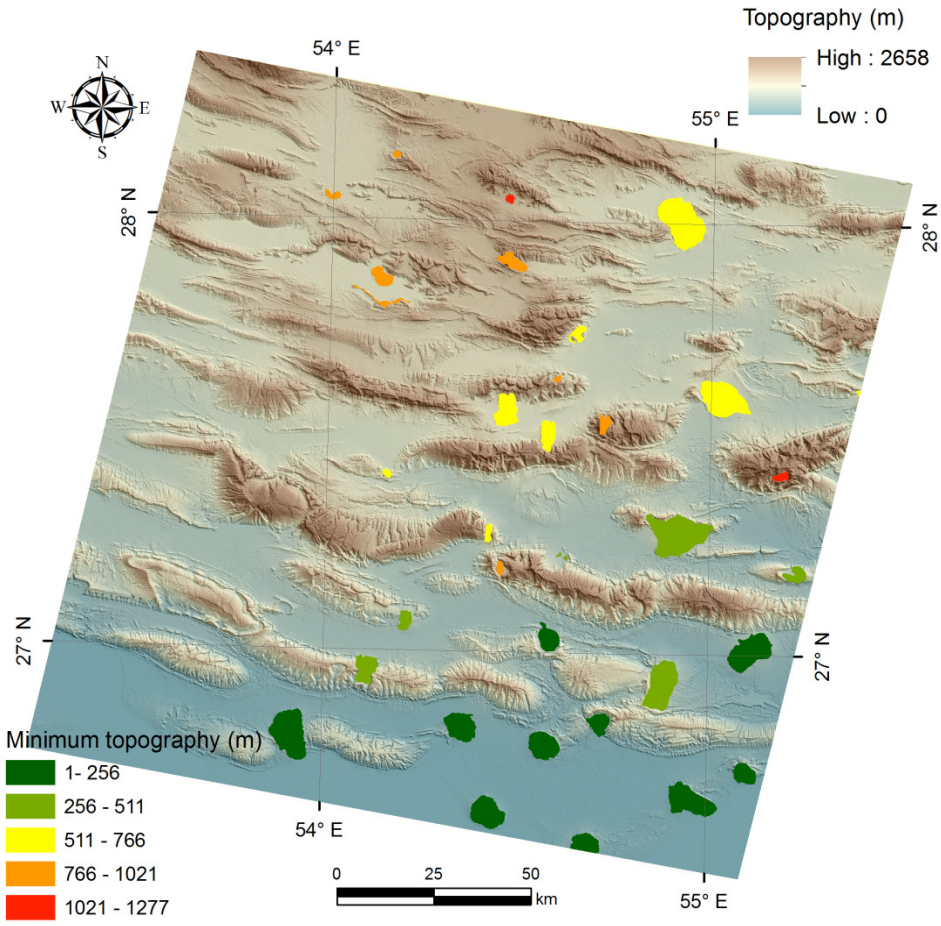

Figure 21. Minimum topography of the salt diapirs in the study area, increasing towards north.

Table 2. Detail information about the altitude of the salt diapirs

name	Longitude	Latitude	Min (m)	Max (m)	Range (m)	name	Longitude	Latitude	Min (m)	Max (m)	Range (m)
1	54.00	28.05	820	993	173	19	54.92	27.28	394	1346	952
2	54.46	28.05	1034	1281	247	20	54.63	27.22	434	537	103
3	54.91	28.00	677	1352	675	21	54.46	27.19	833	1070	237
4	54.47	27.91	941	1708	767	22	55.23	27.19	349	939	590
5	54.13	27.86	775	1273	498	23	54.21	27.07	344	998	654
6	54.14	27.81	782	1214	432	24	54.59	27.03	248	568	320
7	54.65	27.74	682	1097	415	25	55.11	27.01	207	816	609
8	54.60	27.64	874	1306	432	26	54.11	26.95	304	1491	1187
9	55.03	27.60	516	941	425	27	54.88	26.93	317	857	540
10	54.46	27.56	717	1415	698	28	54.72	26.84	64	549	485
11	54.72	27.53	979	1999	1020	29	54.36	26.83	14	235	221
12	54.57	27.51	701	1358	657	30	53.92	26.80	3	709	706
13	54.16	27.41	700	1020	320	31	54.58	26.78	57	571	514
14	55.19	27.42	1277	1999	722	32	55.10	26.73	6	435	429
15	55.41	27.59	514	1014	500	33	54.96	26.66	1	308	307
16	54.42	27.27	651	1292	641	34	54.43	26.63	11	367	356
17	54.61	27.23	432	511	79	35	54.69	26.56	85	533	448
18	54.60	27.23	457	533	76	36	54.16	28.15	913	1290	377

7. DISCUSSION

However, the land surface isotherm maps and the temperature of each individual diapir are acquired for three different years (1987, 2000, and 2006) but in addition the result of this study can be used for two main purposes. Initially, the land surface temperature maps and distribution of the local thermal anomalies and in the arid plains let us to investigate the influence of different rock units on the surface temperature. The second main objective of this study is to estimate a relative movement of the salt diapirs and locate thermal anomalies. The warmer salt diapirs also represent the high rate of the salt extrusion and subsequently imply to the high rate of deformation and large tectonic activity. In the following section, we will explain these results in details.

7.1 THERMAL ANOMALIES

The result of the remote sensing study based upon thermal band of the Landsat images show that the plains are warmer regions to compare with low elevated regions (Figures 6, 10 and 14). As we know, the plains are drained by river systems and cause high rate of moisture in the plains to compare with mountainous regions, and therefore they let to probable thermal anomalies. Although the moisture can result to a warmer regions in the plains, but it is not the case in the Zagros. The annual precipitation rate shows that the western part of the study area receive 20 to 25 cm of rainfall per year and almost zero in the western sector (Figure 22). The northeastern thermal anomaly is constant in the three images (April 1978, May 2000 and March2006) and has almost 1000 meters elevation to compare with the

southern plains. In fact, we expect to have lower temperature in such a plain to compare with the southern plains (150 km towards south) (Figures 23, 24 and 25). Furthermore, the temperature of the atmosphere drops down almost 7 degrees in this region compared with the southern plains next to the Persian Gulf coast. Interestingly, almost all of the thermal anomalies overlap with the salt diapir locations and their adjacent plains (Figures 23, 24 and 25).

The strong link between low amounts of the precipitation, higher altitude and presence of the salt diapir with high thermal conductivity with the thermal anomalies in the plains shows the strong influence of the salt in the land surface temperature in the Zagros region. However, it is worth noting that the distribution of the villages in this region is controlled mostly by the land surface temperature (Figures 26 and 27). Most of the villages, as an excellent example of tolerable conditions of life, are located in the green zones (32-40°C) and the very hot zones are almost empty of life. This is actually is a nice example to show how land surface temperature and salt thermal anomalies influence on the ecology and the environment! There are clusters of the villages almost close to empty plains with high temperature anomaly (Figure 26).

7.2 SALT DIAPIRS

The obtained maximum and mean surface temperature of the salt diapirs are extrapolated to achieve a simplified isotherm map of the salt diapirs (Figures 28 and 29). These maps correspond to the surface thermal maps, but the interesting point is that the temperature of the salt diapirs increases to towards north. Although the morphology of the salt glaciers also represent that salt diapirs in the northern part are more active, and therefore they could transfer and distribute more heat from the underground to the surface. It is worth noting that, the regional warmth of the salt diapirs increase along with increasing topography towards north, whereas we expect to have colder salt diapirs at the higher altitude in the north (Figure 30). This mismatch between altitude and temperature of the salt diapirs strongly suggest that the diapirs in the northeast of the study area are more active compared with the others. Along with that, these diapirs mostly include salt glaciers and include flow structures at the surface. The location of diapirs also consistent with the large earthquakes (bigger than 6) and represent a high stress accommodated zone (Figure 31).

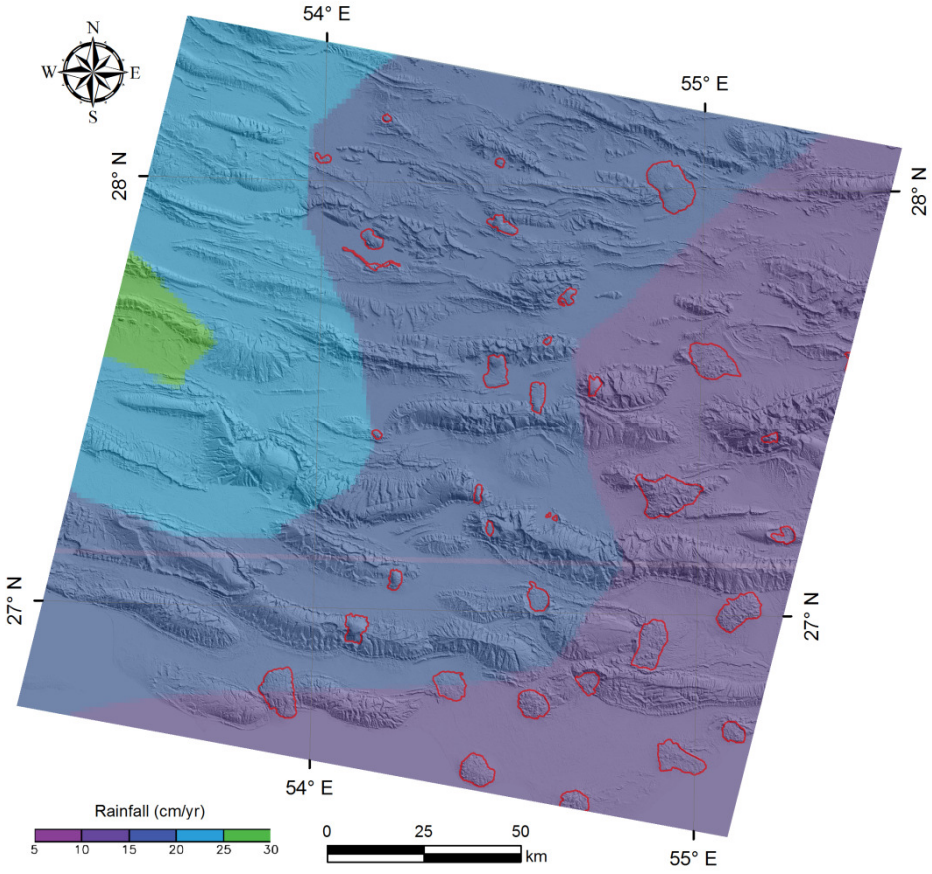

Figure 22. The annual precipitation map of the study area.

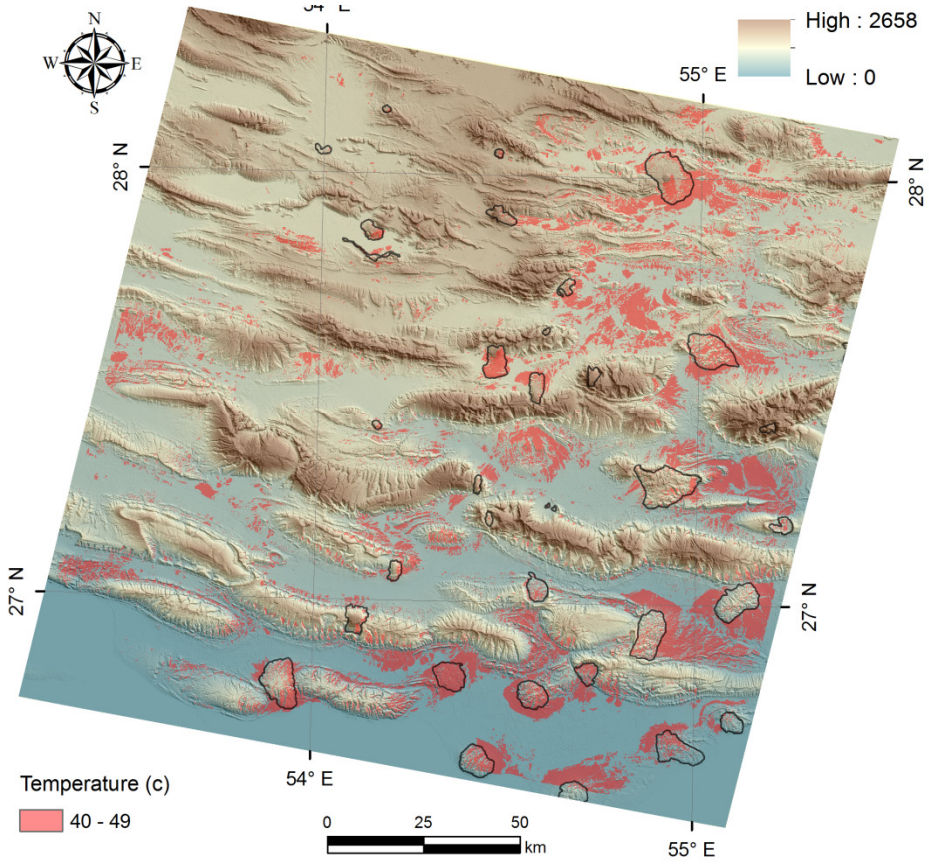

Figure 23. Thermal anomalies along with the location of the salt diapirs, April 1987.

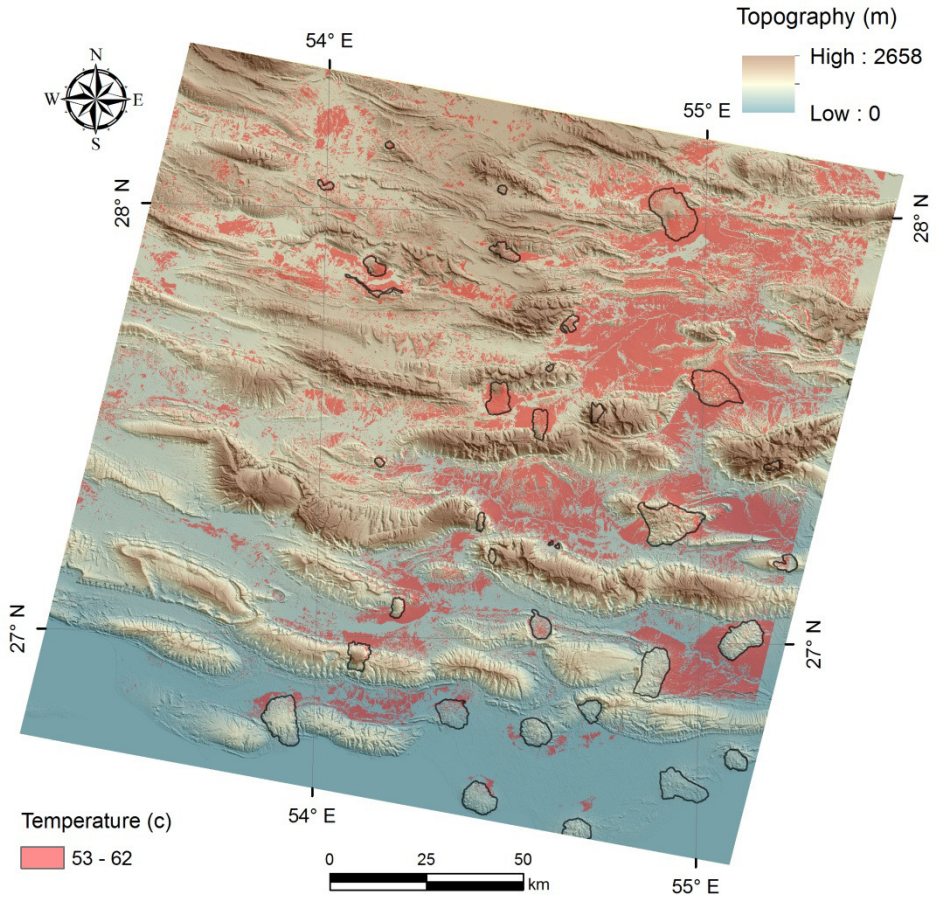

Figure 24. Thermal anomalies along with the location of the salt diapirs, May 2000.

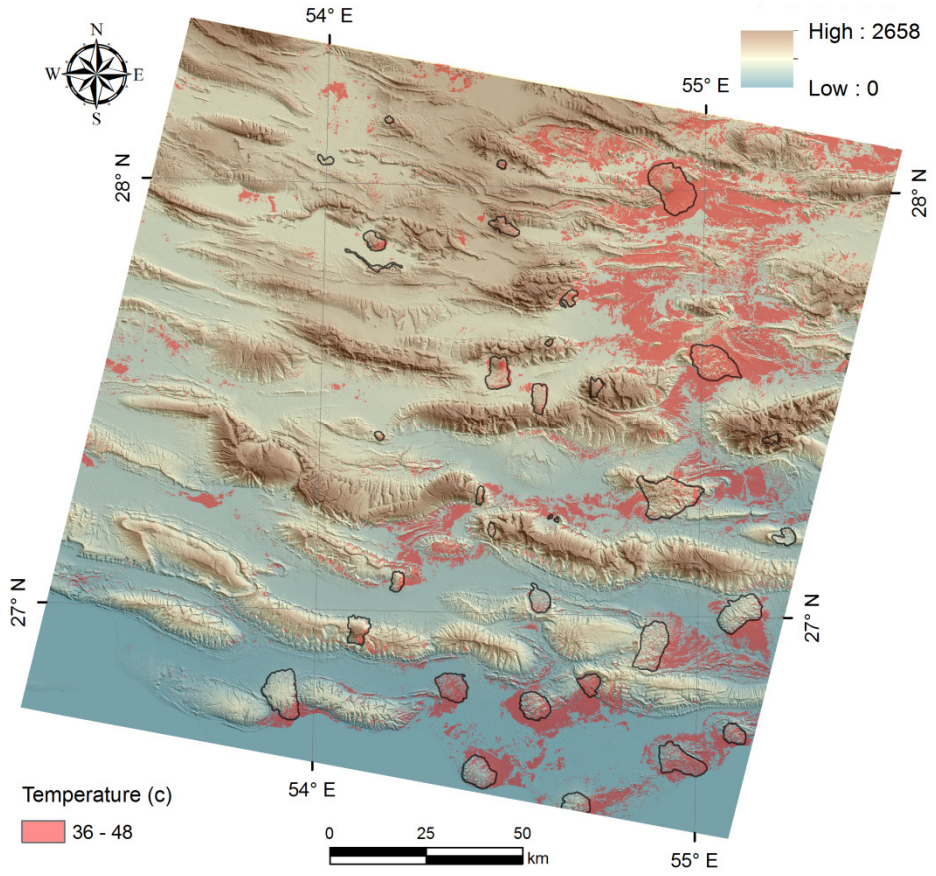

Figure 25. Thermal anomalies along with the location of the salt diapirs, March 2006.

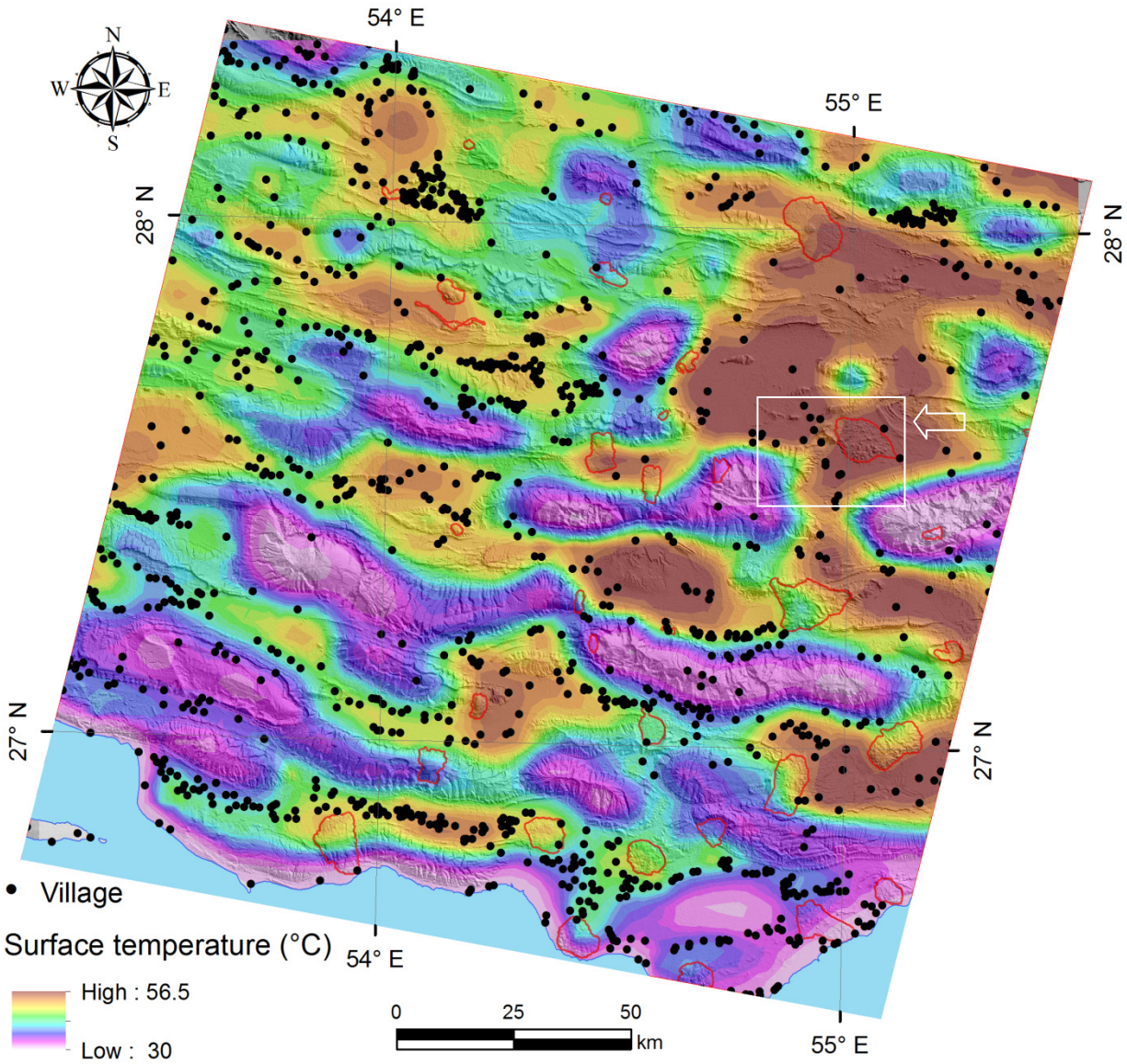

Figure 27. The distribution of the villages in the study area over the isotherm map of May 2000.

Figure 26. An aerial photo from one of the salt diapirs and overview of the region with high thermal anomaly. The salt diapir in the middle of the photo is located in figure 24. View towards west.

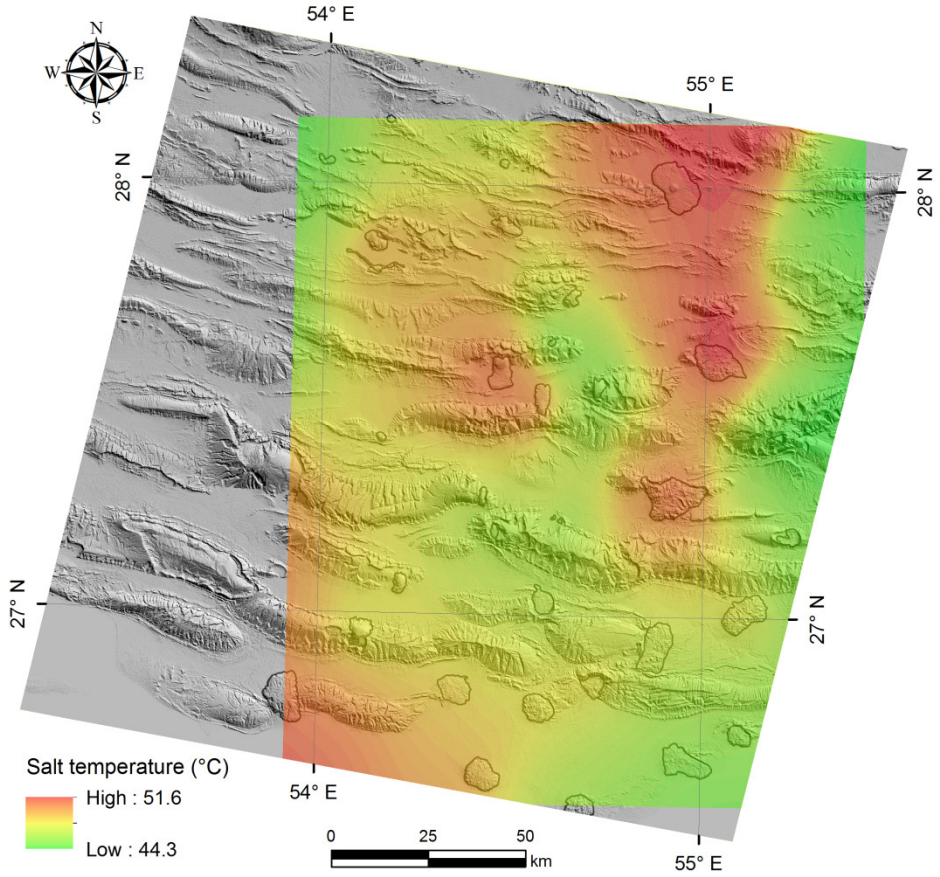

Figure 28. Isothermal map on the basis of the average temperature of maximum temperature of the salt diapirs for three years (1987, 2000 and 2006).

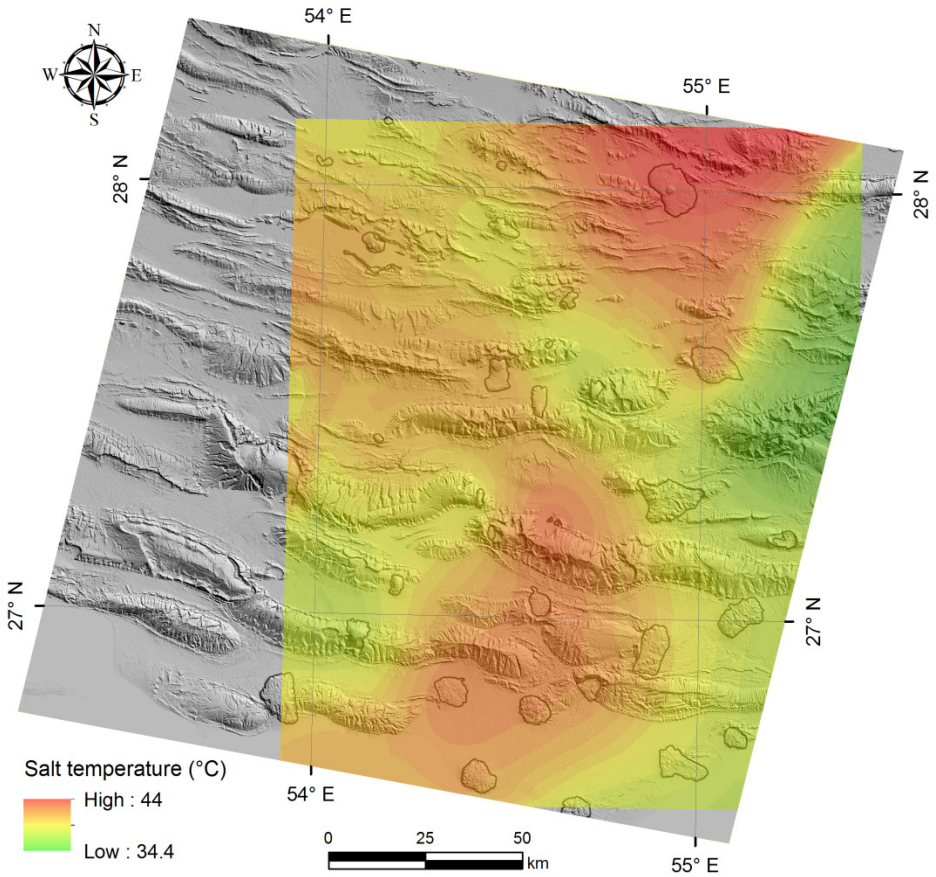

Figure 29. Isothermal map on the basis of the average temperature of the mean temperature of salt diapirs for three years (1987, 2000 and 2006).

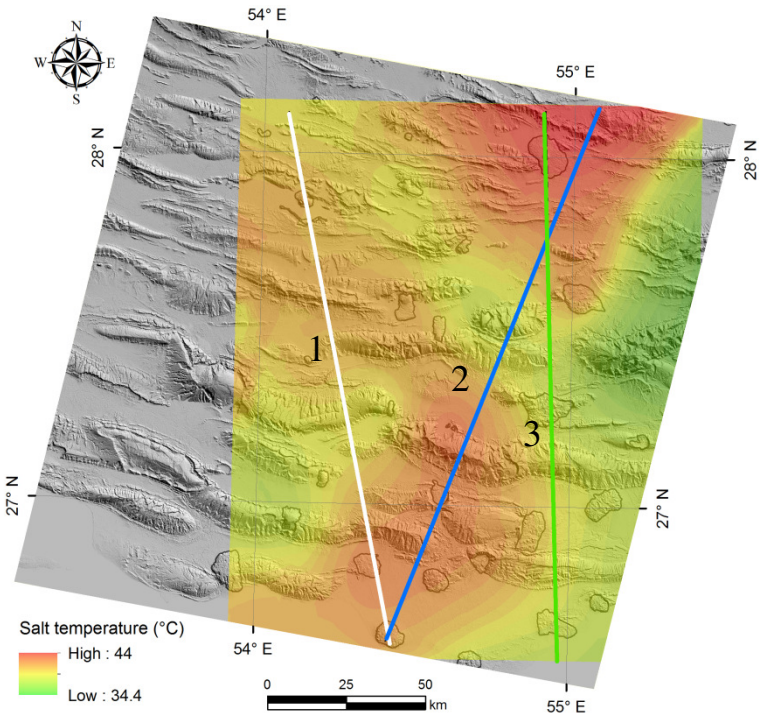

North South

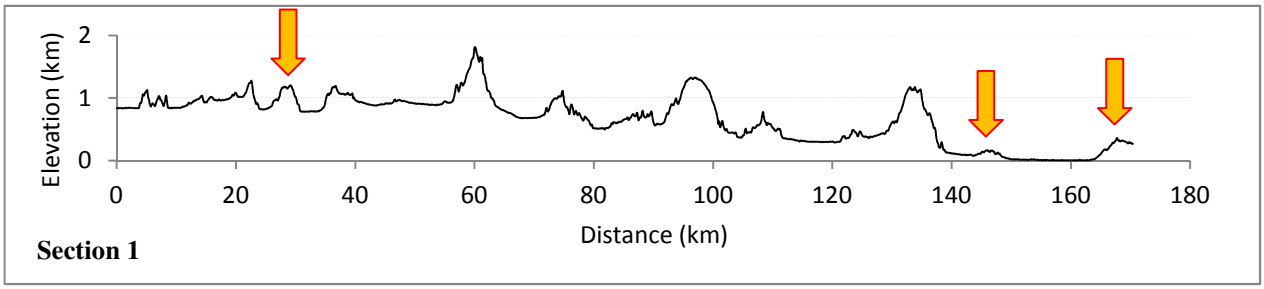

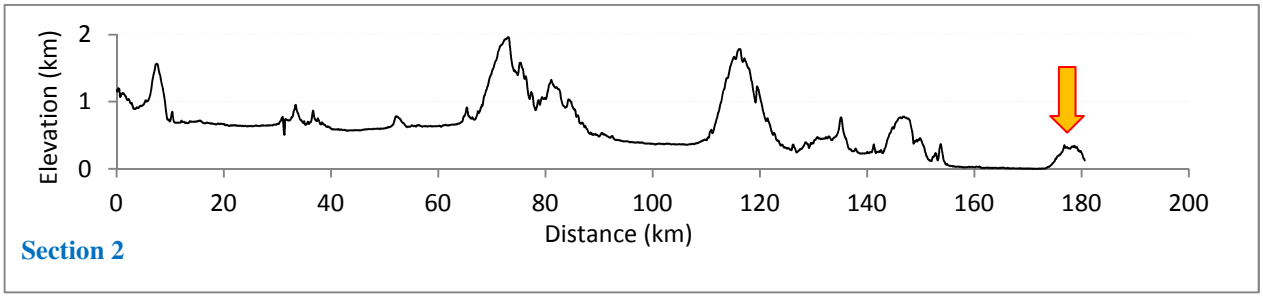

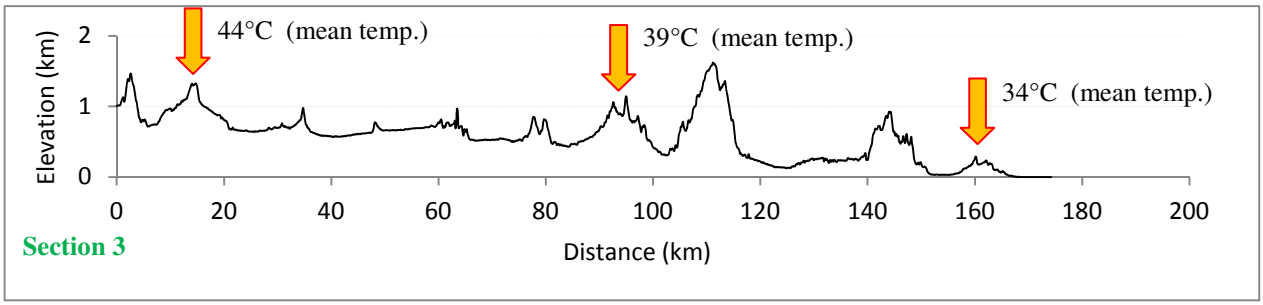

Figure 30.three different topographic section of the study area, the location of the salt diapirs are highlighted.

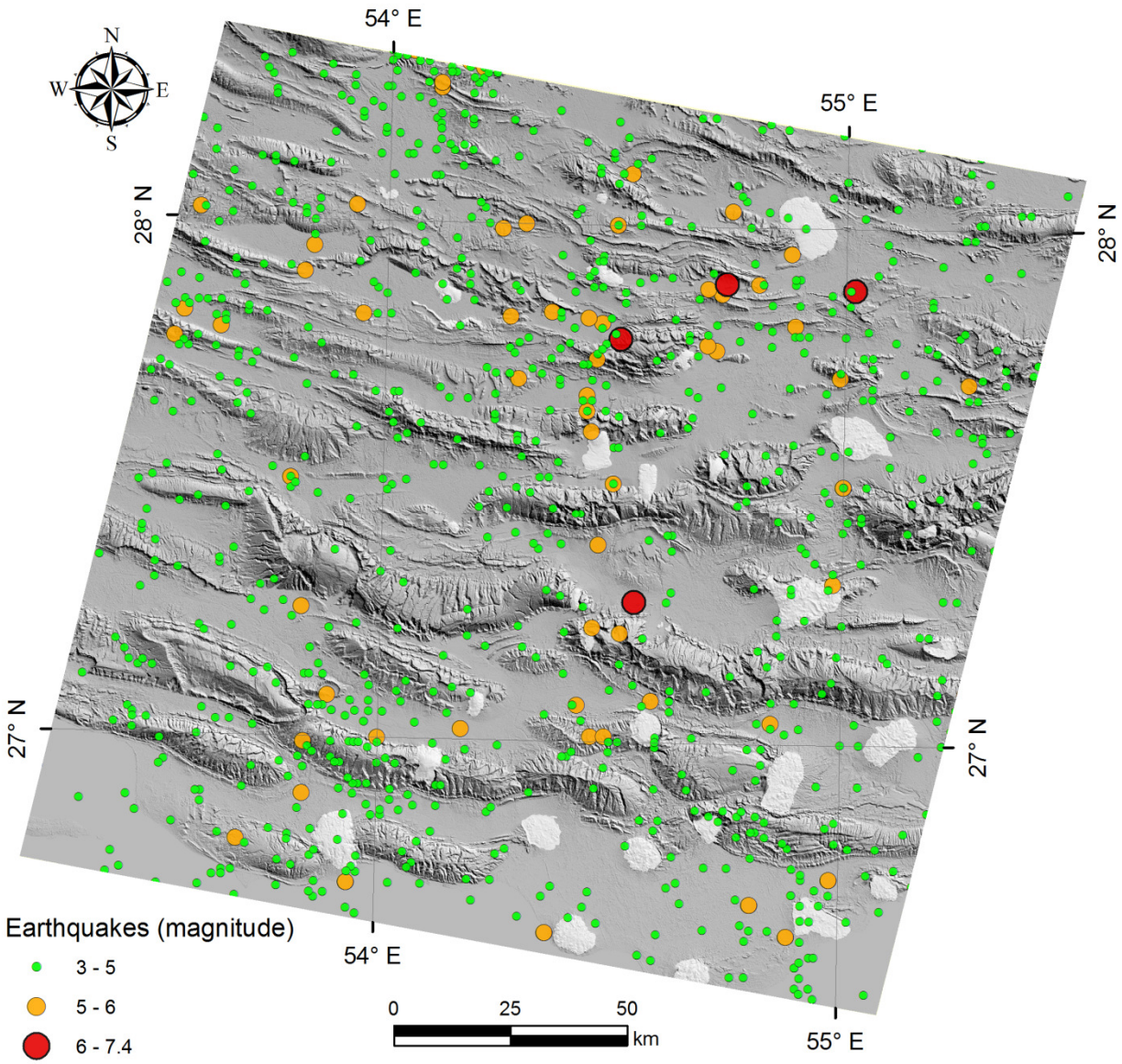

Figure 31. Epicenter of the earth quakes in the study area (1950 to 2012).

8. CONCLUSIONS

This study has provided initial comprehensive investigations into the land surface temperature and the influence of the salt diapirs in the Zagros region. It provides new detailed information concerning thermal anomalies, location of the active salt diapirs and their influence on the regional LST. We have summarized our conclusions in the following sections.

The surface temperature of the northeastern part of the study area represents the constant highest temperature through the last 2 decades. This thermal anomaly at the 1000 meters elevation is surrounded with large and most active salt diapirs. These salt structures are transforming the heat by their extrusion and flow over the surface continuously and have a large impact in the regional land surface temperature. In addition, this study shows that some of the salt structures and the adjacent plains have more than 60°C at the end of spring and more are likely to achieve to higher degrees

in the summer time. They are potential hot spots for further investigations in order to obtain energy from geothermal sources. The salt diapirs located in the northeast of the study area with an average elevation of 900 meters are warmer and most active in this region. The presence of the active salt diapirs with relatively high altitude (to compare with others in the study area) along with larger earthquakes represent that this region locates in a high deformation zone and tectonically active. The relatively rapid extrusion of the salt diapirs transform more heat to the surface from the underground and influence on the heat flux between the Earth's surface and the atmosphere.

7. REFERENCES

Allen, M.B., and Armstrong, H.A., 2008, Arabia -Eurasia collision and the forcing of mid-Cenozoic global cooling: Palaeogeography, Palaeoclimatology, Palaeoecology, v. 265, no. 1-2, p. 52–58, doi: 10.1016/j.palaeo.2008.04.021.

Berberian, M., and King, G.C.P., 1981, Towards a paleogeography and tectonic evolution of Iran: Canadian Journal of Earth Sciences, v. 18, p. 210–265, doi: 10.1139/e81-019.

Beydoun, Z.R., 1991, Arabian plate hydrocarbon geology and potential - a plate tectonic approach. American Association of Petroleum Geologists 33, 77.: American Association of Petroleum Geologists, v. 33, no. 77.

Borel, C., 2008, Error analysis for a temperature and emissivity retrieval algorithm for hyperspectral imaging data: International Journal of Remote Sensing, v. 29, no. 17-18, p. 5029–5045, doi: 10.1080/01431160802036540.

Buettner, K.J.K., and Kern, C.D., 1965, The determination of infrared emissivities of terrestrial surfaces: Journal of Geophysical Research, v. 70, no. 6, p. 1329–1337, doi: 10.1029/JZ070i006p01329.

Chander, G., Markham, B.L., and Helder, D.L., 2009, Summary of current radiometric calibration coefficients for Landsat MSS, TM, ETM+, and EO-1 ALI sensors: Remote Sensing of Environment, v. 113, no. 5, p. 893–903, doi: 10.1016/j.rse.2009.01.007.

Dousset, B., and Gourmelon, F., 2003, Satellite multi-sensor data analysis of urban surface temperatures and landcover: ISPRS Journal of Photogrammetry and Remote Sensing, v. 58, no. 1–2, p. 43–54, doi: 10.1016/S0924-2716(03)00016-9.

Falcon, N.L., 1974, Southern Iran: Zagros Mountains: Geological Society, London, Special Publications, v. 4, no. 1, p. 199 –211, doi: 10.1144/GSL.SP.2005.004.01.11.

Gussow, W.C., 1968, Salt Diapirism: Importance of Temperature, and Energy Source of Emplacement: v. 153, p. 16–52.

Hessami, K., Nilforoushan, F., and Talbot, C.J., 2006, Active deformation within the Zagros Mountains deduced from GPS measurements: Journal of the Geological Society, v. 163, no. 1, p. 143 –148, doi: 10.1144/0016-764905-031.

Lees, G.M., and Falcon, N.L., 1952, The Geographical History of the Mesopotamian Plains: The Geographical Journal, v. 118, no. 1, p. 24–39, doi: 10.2307/1791234.

Murris, R.J., 1980, Middle East: Stratigraphic Evolution and Oil Habitat: AAPG Bulletin, v. 64, doi: 10.1306/2F918A8B-16CE-11D7-8645000102C1865D.

Owen, T.W., Carlson, T.N., and Gillies, R.R., 1998, An assessment of satellite remotely-sensed land cover parameters in quantitatively describing the climatic effect of urbanization: International Journal of Remote Sensing, v. 19, no. 9, p. 1663–1681, doi: 10.1080/014311698215171.

Schott, J.R., and Volchok, W.J., 1985, Thematic Mapper thermal infrared calibration: Photogrammetric Engineering and Remote Sensing, v. 51, p. 1351–1357.

Sepehr, M., and Cosgrove, J.., 2004, Structural framework of the Zagros Fold - Thrust Belt, Iran: Marine and Petroleum Geology, v. 21, no. 7, p. 829–843, doi: 10.1016/j.marpetgeo.2003.07.006.

Snyder, D.B., and Barazangi, M., 1986, Deep crustal structure and flexure of the Arabian Plate Beneath the Zagros collisional mountain belt as inferred from gravity observations: Tectonics, v. 5, no. 3, p. PP. 361–373, doi: 198610.1029/TC005i003p00361.

Takin, M., 1972, Iranian Geology and Continental Drift in the Middle East: Nature, v. 235, no. 5334, p. 147–150, doi: 10.1038/235147a0.

Talbot, C.J., and Alavi, M., 1996, The past of a future syntaxis across the Zagros: Geological Society, London, Special Publications, v. 100, no. 1, p. 89 –109, doi: 10.1144/GSL.SP.1996.100.01.08.

Tatar, M., Hatzfeld, D., Martinod, J., Walpersdorf, A., Ghafori-Ashtiany, M., and Chéry, J., 2002, The present-day deformation of the central Zagros from GPS measurements: Geophysical Research Letters, v. 29, p. 4 PP., doi: 200210.1029/2002GL015427.

Weng, Q., 2009, Thermal infrared remote sensing for urban climate and environmental studies: Methods, applications, and trends: ISPRS Journal of Photogrammetry and Remote Sensing, v. 64, no. 4, p. 335–344, doi: 10.1016/j.isprsjprs.2009.03.007.

Weng, Q., Lu, D., and Schubring, J., 2004, Estimation of land surface temperature–vegetation abundance relationship for urban heat island studies: Remote Sensing of Environment, v. 89, no. 4, p. 467–483, doi: 10.1016/j.rse.2003.11.005.